Universität Stuttgart

Geodätisches Institut

Determination of a gravity field model from one month of CHAMP satellite data using accelerations

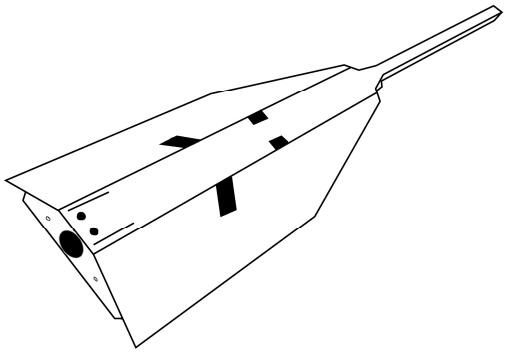

Studienarbeit im Studiengang

Geodäsie und Geoinformatik

an der Universität Stuttgart

Tin Lian Abt

Kopenhagen, Dezember 2004

Betreuer:

Professor Wolfgang Keller
Universität Stuttgart

Professor Carl Christian Tscherning
Københavns Universitet

Declaration

The thesis

"Determination of a gravity field model from one month of CHAMP satellite data using accelerations"

has only been written by the author. No sources have been used other than those indicated within the thesis itself.

Copenhagen, December 2004

Tin Lian Abt

Abstract

A gravity field model has been estimated based on reduced dynamic and kinematic state vectors of CHAMP. Newton Interpolation has been used to calculate accelerations and Least-Squares Collocation to estimate the spherical harmonic coefficients.

During data preprocessing positions and velocities of the reduced dynamic and kinematic state vectors are synchronized so that two corresponding data sets of one month (July 2002) with a sampling rate of 30s are achieved. Observations where the kinematic velocity is rejected due to edge effects or GPS observation discontinuities are deleted in both data sets.

A comparison of the two sets of state vectors shows that the majority of the differences in magnitude of position and velocity are in the range between ± 0.2m and ± 0.5mm/s respectively. Observations outside these boundaries are declared outliers and deleted. This reduces the data sets by approximately 0.7%.

Newton Interpolation approximates the velocity vectors which are transformed into an inertial system by a polynomial. Tests ascertain that the use of seven interpolation points achieves good results. The first derivative with respect to time of these polynomials gives the acceleration vector of each observation.

One-third of the reduced dynamic and kinematic observations have been utilized for the estimation of spherical harmonic coefficients. The Least-Squares Collocation is based on gravity disturbances derived from the magnitudes of accelerations. EGM96 up to a degree and order of 24 is used for the “remove-restore” method so that data become statistically more homogenised.

A comparison of the reduced dynamic and kinematic accelerations to those based on EGM96 up to a degree and order of 360 shows that the kinematic data are more influenced by noise than the reduced dynamic. The standard deviations of differences in accelerations calculated from EGM96 minus reduced dynamic or

kinematic are 0.3mgal and 1mgal respectively.

These results are also reflected in the quality of the spherical harmonic coefficients. The standard deviations of differences in coefficients between EGM96 and reduced dynamic data are always lower than those between EGM96 and kinematic data.

Up to degree 60, both types of standard deviations are lower than the standard deviations of EGM96 coefficients themselves. The estimated gravity field model therefore provides information consistent with EGM96 up to degree 60. The model shows also an improvement with respect to coefficients which are derived by the energy conservation method utilizing the same data.

Table of contents

Table of figures

1 Introduction

1.1 Motivation

Gravity is not a constant. Its magnitude depends on the place and time so that one should refer to gravity as a field instead of as a constant term.

Due to the earth's rotation, the body of the earth is flattened at the poles. This results in different values of gravity especially when one compares the gravity at the poles to the gravity at the equator.
However, the flattening of the earth is not the only impact on the figure of the earth which could otherwise simply be described as an ellipsoid. Varying masses and their different distributions inside the earth as well as different kinds of topography result in a gravity field similar to the one shown in the exaggerated figure 1. Variations over time are caused by the movements of rocks, ice and oceans.

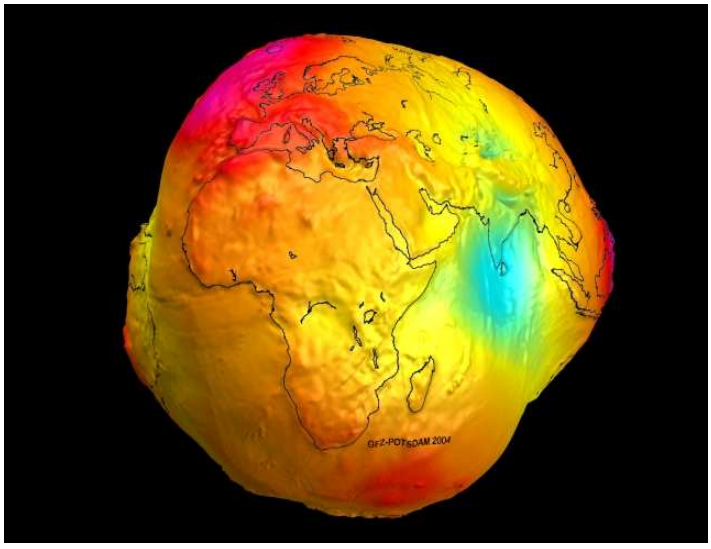

figure 1: exaggerated geoid model © GFZ

The global gravity field forms the basis for various research interests. The knowledge of the gravity field reveals for example information in geophysics about the structure of the earth's continental and oceanic lithosphere. Oceanographer can determine the global ocean circulation which is an indicator for global climate changes while in geodynamics the gravity field is used to observe time varying

phenomena such as the post glacial uplift or the sea level changes [Seeber 1993]. In geodesy, the equipotential surface of the gravity field defines a reference system of heights.

Several gravity field models have been obtained from a combination of satellite tracking data, local terrestrial gravity measurements and satellite altimetry data.
Inaccuracies occur in case of the satellite tracking data as the utilised satellites have been designed for purposes other than gravity measurements. These satellites have therefore a high altitude. The higher a satellite, the lower the signal which means that less information about the gravity field can be obtained.
Terrestrial gravity measurements and satellite altimetry, on the other hand, have the disadvantage that they are not globally distributed. Terrestrial gravimetry only takes place at a local level while the altimeter data are restricted to oceans.

In order to solve these problems three different satellite missions have been designed, CHAMP, GRACE and GOCE. They all have in common a low earth orbiting satellite. Due to the low altitude an improvement of the accuracy and resolution of existing gravity field models can be achieved. This improvement is essential for all fields of research interests. The three satellite missions have also the advantage that they each cover almost the whole earth so that problems of combining different satellite tracking data sets are dissolved.

1.2 Task and Structure

Within the described background the task of this study thesis is the computation of a gravity field model using data from a low orbiting satellite. Furthermore, this gravity field model should be based on the accelerations of the CHAMP satellite.

A common way of deriving accelerations is to compute either the second derivative of the positions or the first derivative of the velocities. Differentiating means that two sequent points of an orbit are included in the computation. However, in order to increase the accuracy of the accelerations, more than two points should be included. This improvement can be achieved by using Newton Interpolation.

A different approach for the estimation of a gravity field model is based on the energy conservation method which was carried out within an earlier project. This method does not use the accelerations and should therefore be less influenced by noise.

One more task of the study thesis is to draw a comparison between the gravity field model based on the energy conservation method and the gravity field model which will be derived from accelerations.
This comparison will show if the gravity field model based on accelerations is similar to or even better than the gravity field model based on energy conservation. It will also be possible to determine which problems depend on the satellite measurements and which problems result from a certain method.

The method of resolution in this study thesis is therefore in a first step to preprocess and compare two different CHAMP data sets, *reduced dynamic* and *kinematic*. Second, accelerations of each data set will be computed by Newton Interpolation and finally Least-Squares Collocation will provide the estimated gravity field. The *reduced dynamic* and *kinematic* gravity field models will be compared to the gravity field model which is based on the energy conservation method (Chapter 6).

The course of action is illustrated in figure 2.

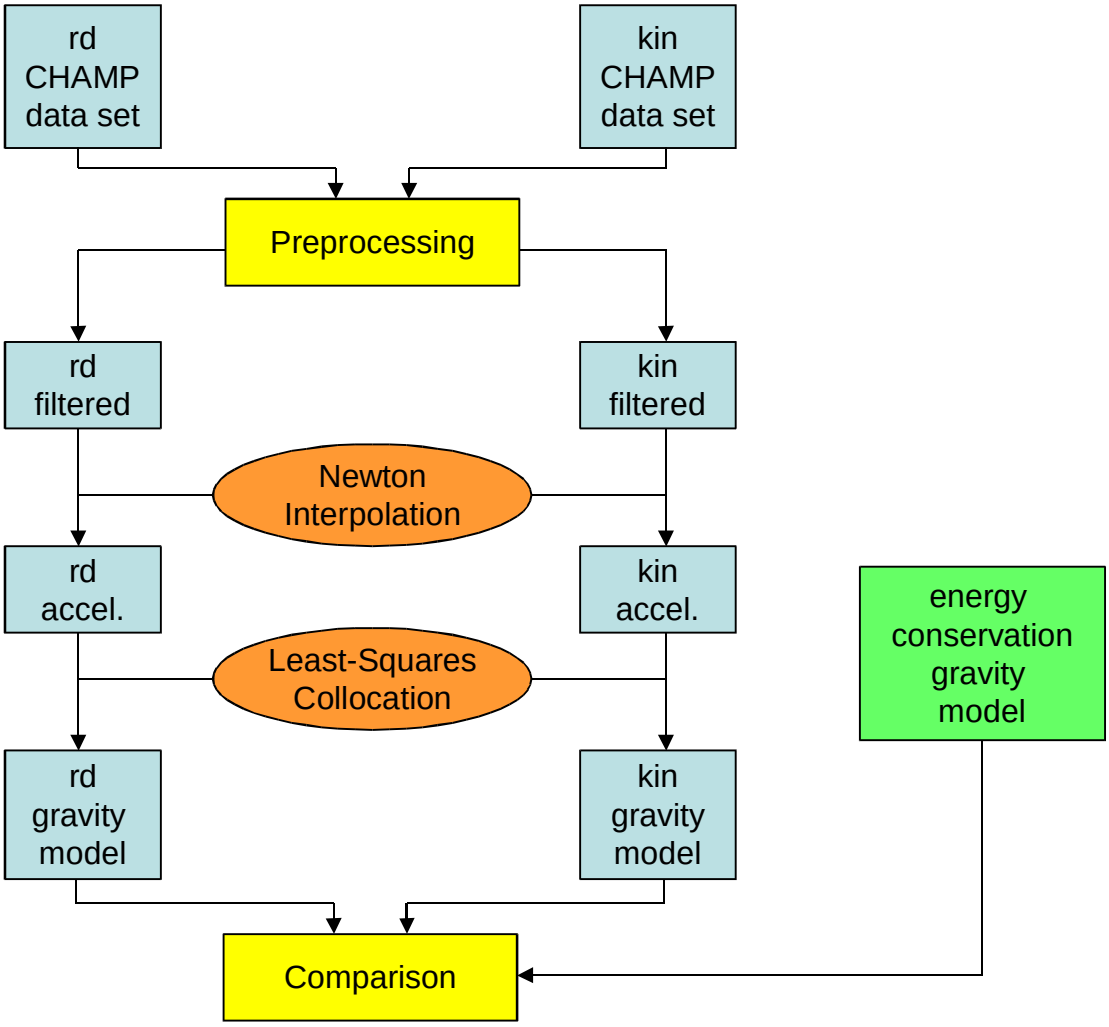

figure 2: structure of proceedings (rd: reduced dynamic, kin: kinematic)

Chapter 2 gives a short summary of the basic properties which occur within this study as well as an introduction to the satellite mission CHAMP.

The data preprocessing step is described in Chapter 3.

In Chapter 4 and 5 one can read about the main computational steps, namely the Newton Interpolation and the Least-Squares Collocation.

Some basic information about the energy conservation method are given in Chapter 6.

Chapter 7 presents the results of the computations which are carried out in Chapter 4 and 5.

Chapter 8 finally gives the conclusion and some ideas of what might be done in future work.

2 High-resolution gravity field

2.1 Basic properties of the gravity field

This section gives a short introduction to some basic properties of the gravity field. Only those properties which occur within this study are described.

Gravitational potential

A gravity field is characterized by its gravitational potential *V*. This fundamental property may be expressed by equation 2.1 [Mortiz 1980] where *P* is a point given in x, y and z coordinates, *Q* is a point inside the earth which at the same time presents the centre of the volume element dv_Q and *l* represents the distance between the two points *P* and *Q*. *G* stands for the Newtonian gravitational constant (equation 2.2).

$$V(P) = G \iiint_{earth} \frac{\rho(Q)}{l} dv_Q \tag{2.1}$$

$$with \quad G = 6.672 * 10^{-6} \left[\frac{m^3}{s^2\ kg} \right] \tag{2.2}$$

Figure 3 illustrates the parameters of equation 2.1. However, considering a global scale this equation is only valid in theory as it requires full knowledge of the detailed density distribution *ρ(P)* within the earth. These details are unknown and cannot be easily modelled.

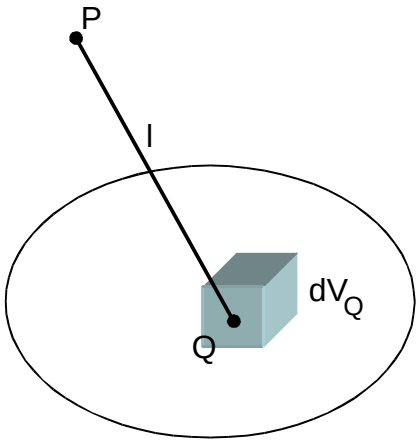

figure 3: relationship between point P and Q

In practice the advantage is used that the gravitational potential is a harmonic function and can therefore be expressed as a series expansion of spherical harmonic coefficients. Equation 2.3 shows this expansion which also gives a solution to Laplace's differential equation (equation 2.4) in the exterior space.

$$V(P) = \frac{GM}{r_p}\left[1 + \sum_{i=1}^{\infty}\left(\frac{a}{r_p}\right)^i \sum_{j=-i}^{i} \bar{P}_{ij}(\sin(\varphi_p)) \begin{Bmatrix} \cos(j\lambda_p)\, c_{ij} \\ \sin(j\lambda_p)\, s_{ij} \end{Bmatrix}\right] \quad \begin{matrix} if \quad j \geq 0 \\ if \quad j < 0 \end{matrix} \tag{2.3}$$

$$\Delta V = 0 \tag{2.4}$$

V(P) defines the gravitational potential of an arbitrary point *P* with the spherical coordinates *λ,φ,r. M* is the mass of the earth while r_p being the radial distance of the point *P*. The parameter *a* stands for the semi-major axis of the reference ellipsoid, $\bar{P}_{ij}(\sin(\varphi_p))$ are the fully normalized Legendre functions of the first kind and finally c_{ij} and s_{ij} present the spherical harmonic coefficients. The set of these coefficients characterises the gravity field.

Gravity potential and gravity

The gravity potential *W* (equation 2.5) contains the sum of the gravitational potential *V* and the centrifugal potential *Φ* (equation 2.6) which is caused by the rotation of the earth. Here *ω* stands for the constant angular velocity of the earth.

$$W(x,y,z) = V(x,y,z)+\Phi \tag{2.5}$$

$$with \quad \Phi = \frac{1}{2}\omega^2(x^2+y^2) \tag{2.6}$$

The gradient of *W* is called gravity vector and has the direction of the vertical or plumb line [Moritz 1980]. Gravity *g* is the magnitude of the gravity vector (equation 2.7).

$$g = \|grad\ W\| \tag{2.7}$$

The geoid which approximates the mean sea surface has a constant *W* and is at every point perpendicular to the gravity vector.

Normal potential and normal gravity

The gravity potential *W* of the earth can be approximated by a normal potential *U* of a reference surface such as a sphere or an ellipsoid. The reference surface of *U* is also an equipotential surface like the geoid.

U is defined as a sum containing the normal gravitational potential $\bar{V}$ and the centrifugal potential Φ (equation 2.8).

$$U(x,y,z) = \bar{V}(x,y,z)+\Phi \tag{2.8}$$

The gradient of *U* is called normal gravity vector. Normal gravity γ is the magnitude of the normal gravity vector (equation 2.9).

$$\gamma = \|grad\ U\| \tag{2.9}$$

Anomalous potential

The subtraction of the normal potential *U* from the gravity potential *W* is called anomalous potential *T* (equation 2.10). It presents the residual of the gravity

potential which cannot be approximated by the reference surface.

$$T = W - U \tag{2.10}$$

The centrifugal potential Φ is eliminated by the subtraction of equation 2.10 under the assumption that gravity and normal potential both contain the same constant angular velocity ω of the earth.

Gravity anomaly and gravity disturbance

Considering equation 2.3 to equation 2.10 potentials always refer to the same point P. However, when introducing the gravity anomaly it is important to distinguish between the point *P* on the geoid and a corresponding point *Q* located on the reference surface. The normal gravity vector in *P* intersects the reference surface in *Q* (figure 4) whereby the normal potential in *Q* equals the actual potential in *P*.

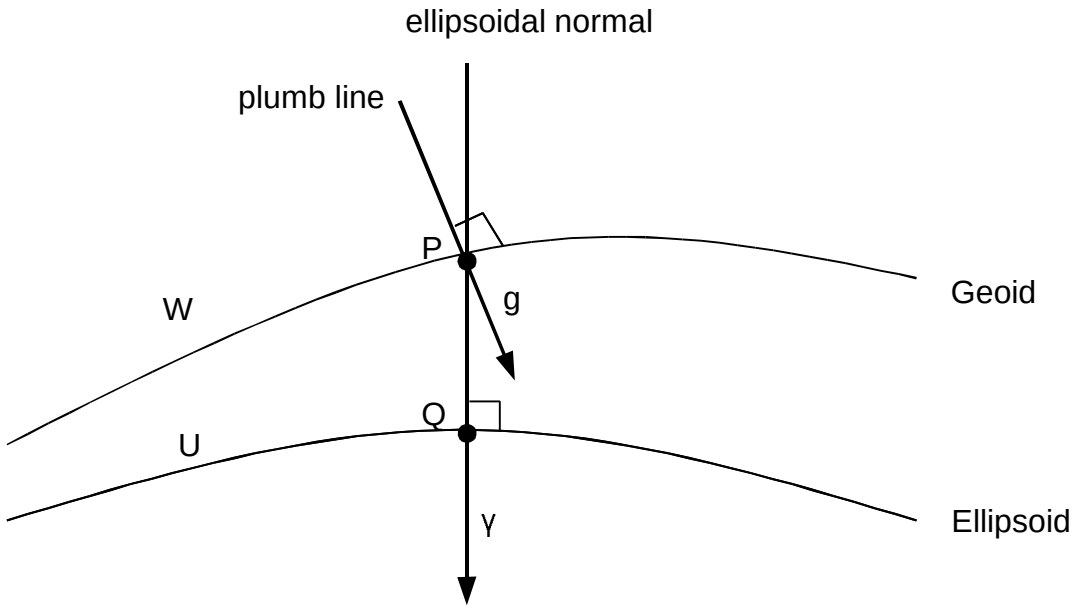

figure 4: geoid and reference ellipsoid, compare [Moritz 1980]

The gravity anomaly Δg is defined as the difference between the measured gravity in *P* and the normal gravity in *Q* (equation 2.11).

$$\Delta g = g(P) - \gamma(Q) = -\frac{\partial T(P)}{\partial r_P} - \frac{2}{r}T \tag{2.11}$$

The gravity disturbance δg on the other hand is defined as the difference between measured gravity and normal gravity both referring to the point *P* (equation 2.12).

$$\delta g = g(P) - \gamma(P) = -\frac{\partial T(P)}{\partial r_P} \tag{2.12}$$

Equation 2.11 and equation 2.12 also show how gravity anomaly and gravity disturbance are related to the anomalous potential *T*.

Spherical coordinates

Since the position vectors of CHAMP are initially given as x, y and z components these coordinates have to be transformed into the spherical longitude λ, latitude φ and radius *r* at some points. This transition is realised by equation 2.13 to 2.15.

$$\lambda = \arctan\left(\frac{y}{x}\right) \tag{2.13}$$

$$\varphi = \arctan\left(\frac{z}{\sqrt{x^2+y^2}}\right) \tag{2.14}$$

$$r = \sqrt{(x^2+y^2+z^2)} \tag{2.15}$$

Outside the earth

The above formulas of this section are valid for a point *P* on the surface of the earth as well as for a point *P* at satellite altitude. However, one has to consider that a satellite is usually described in an inertial frame where the rotation of the earth has no influence and therefore no centrifugal forces occur.

2.2 CHAMP mission

This section is based on the information given by the GeoForschungsZentrum (GFZ) website [GFZ 2004] where also further details about CHAMP can be found.

The abbreviation of the satellite mission CHAMP stands for CHAllenging Minisatellite Payload. This mission is managed by GFZ in Potsdam.

figure 5: model of CHAMP satellite © Astrium

The main task of the satellite (figure 5) which was launched on the 15th of July 2000 is to collect data for geoscientific and atmospheric research. The aim is to create a global model of the earth which leads to a better understanding of the structure and composition of this planet. This understanding refers to an earth not only being static but also being a dynamic system that varies over time (compare section 1.1).

All fields of research interests can be divided into three parts: 1. Gravity, 2. Magnetics and 3. Atmosphere and Ionosphere. In order to obtain the required

data the payload of the CHAMP satellite contains a GPS receiver, a laser retro reflector, a three-axes accelerometer, a magnetometer, a star sensor and an ion drift meter.

As the task of this study is the modelling of a gravity field, only data from the first classification are needed. Via satellite-to-satellite tracking (SST), the GPS receiver continuously monitors the orbit of the CHAMP satellite. Perturbations of this orbit indicate varying gravity. At the same time, the high-precision accelerometer provides measurements of the non-gravitational accelerations. Non-gravitational accelerations are those which are not caused by the attraction of the planet but by atmospheric drag (see section 4.5) for example. The GPS and accelerometer data are used to model the gravity field of the earth.

The CHAMP satellite has an inclination of 87° which corresponds to an almost circular and near-polar orbit. This has the advantage of getting an almost homogeneous and complete global coverage of the earth.

The initial satellite altitude is set to around 454km. Several considerations are taken into account when this altitude was chosen.
First, the mission should last for at least five years so that the earth can be observed as a dynamic system. Due to atmospheric drag and solar activity the altitude of the satellite decreases over time. A certain initial altitude is therefore necessary to guarantee a lifetime of several years before the satellite enters the atmosphere.
Second, for magnetic research, the chosen altitude is ideal but for gravity purposes a lower initial altitude would be preferred. Geodesists and geophysicists are in particular interested in the high-frequency information of a low orbiting satellite because the low-frequency information have already been observed many times by former missions utilising satellites at higher altitudes.
Third, scientists who analyse the atmosphere and ionosphere need an initial altitude at least above the atmospheric layers and would desire an even higher satellite altitude.

The initial CHAMP altitude is relatively low but it is also a compromise between the interests of different fields of research.

The CHAMP satellite has a mean period of 93.55min which results in approximately 15.4 revolutions per day. During this time, 141MByte of data are collected consisting mainly of research data but also of house-keeping data. These data are downloaded to the two ground stations of the German Aerospace Center (DLR) in Neustrelitz and Weilheim. The raw data are then processed at GFZ Potsdam so that different products depending on the level of processing can be provided for scientific research.

3 Preprocessing of CHAMP data

3.1 *Reduced dynamic* and *kinematic* data

CHAMP data files consist of information about the satellite orbit given in form of state vectors. A state vector includes the position vector and the velocity vector of the CHAMP satellite given according to the three components in x, y and z direction. The three coordinates refer to the earth-fixed Conventional Terrestrial System CTS.

Within this work two different sets of CHAMP data have been used, *reduced dynamic* and *kinematic*. The *reduced dynamic* data were obtained from the GeoForschungsZentrum Potsdam [GFZ 2004] while the *kinematic* data were kindly provided by Lorant Földvary at the “Institut für Astronomische und Physikalische Geodäsie“ (IAPG) of the “Technische Universität München“ (TUM).

The main difference between these two data sets is that the *kinematic* data are only based on GPS measurements while the *reduced dynamic* data also include some a priori information derived from several already existing gravity field models.

On one hand it is certain that the kinematic data are raw and not influenced by any other prior observations but on the other hand one has also to consider the fact that the GPS measurements cause noise on the data.

The time interval for *kinematic* and *reduced dynamic* observations are 30s and 10s respectively hence the *reduced dynamic* observations are able to represent the orbit of the satellite in more details.

In order to benefit from both observation methods it is recommended to use both data sets. If these sets are compared to each other it will be possible to decide whether certain observations are likely to be more accurate or not. Errors can be detected more easily if there are two sources for each state vector. However, a

synchronization of the two data sets has to be carried out before they can be compared to each other.

3.2 Data formats

The *reduced dynamic* data are given in the CHAMP Orbit Format (CHORB) which is a standard format as shown by the list below in which every tag of the list is column tabulated.

- Time tag (10^{-1} d since J2000.0)
- Time tag (10^{-6} s since 0 hours TT)
- X coordinate of position (10^{-3} m)
- Y coordinate of position (10^{-3} m)
- Z coordinate of position (10^{-3} m)
- X coordinate of velocity (10^{-7} m/s)
- Y coordinate of velocity (10^{-7} m/s)
- Z coordinate of velocity (10^{-7} m/s)
- Roll angle (10^{-3} deg)
- Pitch angle (10^{-3} deg)
- Yaw angle (10^{-3} deg)
- Neutral gas density (10^{-16} g/cm^3)
- Maneuver flag (M = yes, else blank)
- Land/Water flag (L = Land, W = Water)
- Ascending/descending arc flag (A = ascending, D = descending)
- Eclipse flag (E = satellite in earth's shadow, else blank)

This trajectory record description can be found on the GFZ Potsdam website [GFZ 2004]. The data are stored in several ASCII files of which each includes approximately 24 hours of measurements. The measurement starting time can vary from file to file.
In this research work only the day, time, position and velocity are a matter of interest and therefore the last columns of the files are ignored.

The *kinematic* data,on the other hand, are given by the following format.

- Year
- Month
- Day
- s since 0 hours of the day (GPST)
- X coordinate of position (m)

- Y coordinate of position (m)
- Z coordinate of position (m)
- X coordinate of velocity (m/s)
- Y coordinate of velocity (m/s)
- Z coordinate of velocity (m/s)
- Velocity flag (0 = accepted, 1 = rejected)

The contents are stored in a tabulated form and only in one ASCII file which includes data of one month (July 2002).

As the *reduced dynamic* data are provided for a period of one year (2002), the corresponding files to July 2002 need to be selected.

3.3 Synchronisation

In order to analyse corresponding observations of the same time step, the type of data and the time frames of both data sets have to be the same. For this reason, the days in the *reduced dynamic* data set which are given as Julian days since J2000.0 are converted into days of the month as given by the *kinematic* orbit format. While the *kinematic* orbit is observed in GPS Time (GPST) the *reduced dynamic* observations are given in Terrestrial Time (TT). Both time frames can easily be transformed into the common civil time Coordinated Universal Time (UTC) by equation 3.1 and equation 3.2.

$$UTC = GPST - 13\,s \tag{3.1}$$

$$UTC = TT - 64.148\,s \tag{3.2}$$

As the *reduced dynamic* data sampling rate is three times higher than the *kinematic* data sampling rate (10s versus 30s) no more than one third of the *reduced dynamic* observations can be taken. Nevertheless, it is not enough to simply compare every third state vector of the *reduced dynamic* files to every state vector of the *kinematic* file. Problems arise with the measurement gaps in the *reduced dynamic* data. Interruptions of the measurement sequence are likely to occur between the change of two ASCII files or between the change of two days.

In order to avoid errors, the day and the time of two corresponding state vectors, *reduced dynamic* and *kinematic*, must be the same. Assuming that the chosen files all belong to the same year and month of that year. During the preprocessing only those state vectors are therefore compared for which equation 3.3 is true.

$$\|\Delta day\| < 1\,d \;\wedge\; \|\Delta time\| < 1\,s \tag{3.3}$$

$$with \quad \Delta day = day_{reduced\ dynamic} - day_{kinematic}$$
$$\Delta time = time_{reduced\ dynamic} - time_{kinematic}$$

The synchronised data start on the 2nd of July 2002 as there are no *reduced dynamic* data on the 1st of July 2002.

Gaps do not only exist in the *reduced dynamic* observations but also in the *kinematic* data set.

These gaps occur in the *kinematic* velocity estimation due to GPS observation discontinuities and edge effects. The flags of the velocity refer to the velocity estimation process and determine whether the velocity should be accepted or rejected. All observations for which the velocity should be rejected, that means for which the flag equals one, need to be deleted. The corresponding *reduced dynamic* observations are deleted as well.

3.4 Comparison of data sets

So far up to this extent, two synchronized ASCII files of the same length have been created. One consists of the filtered *reduced dynamic* orbit data and the other of the filtered *kinematic* orbit data. It is now possible to calculate the difference in position and velocity of both observation methods.

The differences are calculated with respect to the x, y and z component of each position and velocity vector (equation 3.4 and equation 3.5).

$$\begin{bmatrix} \Delta x & \Delta y & \Delta z \end{bmatrix}_{position} = \begin{bmatrix} x & y & z \end{bmatrix}_{reduced\ dynamic} - \begin{bmatrix} x & y & z \end{bmatrix}_{kinematic} \quad (3.4)$$

$$\begin{bmatrix} \Delta vx & \Delta vy & \Delta vz \end{bmatrix}_{velocity} = \begin{bmatrix} vx & vy & vz \end{bmatrix}_{reduced\ dynamic} - \begin{bmatrix} vx & vy & vz \end{bmatrix}_{kinematic} \quad (3.5)$$

The results of the above subtractions show that the differences are of similar sizes over the whole period. Most of the differences in position are not bigger than ±1dm and differences in velocity have the quantities of approximately ±1mm/s. However, there is a notable deviation for the last twelve hours of the month. On the 31st of July 2002 at noon time, differences start to increase towards the end of the day. Figure 6 and figure 7 both illustrate the oscillating growing of the difference in position and velocity respectively.

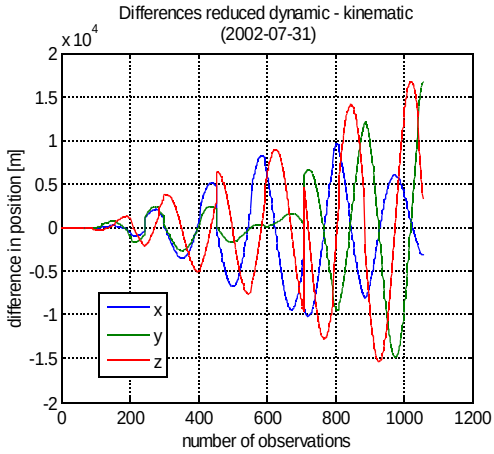

figure 6: differences in position (2002-07-31)

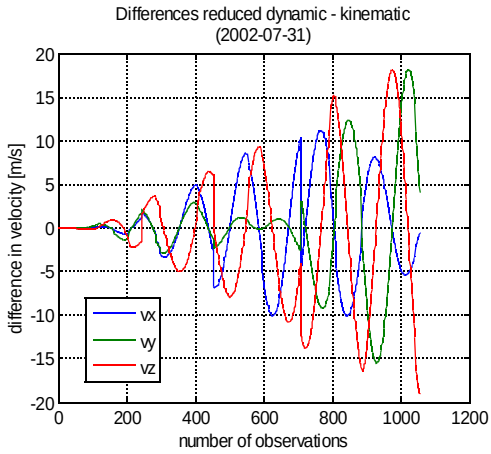

figure 7: differences in velocity (2002-07-31)

As these differences become extremely large (up to 20km in position) there seem to be some problems with one of the data files.

Within an earlier project scale factors for the *reduced dynamic* non-gravitational accelerations have been computed. It was found out that approximately at the same time as mentioned above (last twelve hours of July 2002) the scale factors suddenly turned to be negative. Under consideration of those investigation it can be concluded that there is a defect in the *reduced dynamic* observations.

Nevertheless, the 31st of July 2002 is completely taken out of the data sample so that further investigations only refer to the period between the 2nd and the 30th of July 2002.

The following table 1 to table 3 present the maximum, minimum and average

difference in position and its empirical standard deviation over a period of one day, one week and one month.

As expected, the extreme values (maximum and minimum) are the higher the longer the period becomes. However, the average difference decreases as more data are compared. One can therefore assume that there is a stability in the differences over a long period.

Differences in position [m] (*reduced dynamic – kinematic*)

table 1

1 day	***x***	***y***	***z***
max	0.12190	0.12700	0.13790
min	-0.13480	-0.17510	-0.09240
mean	0.01224	-0.02325	0.02350
std	0.05850	0.062095	0.03316

table 2

1 week	***x***	***y***	***z***
max	0.27810	0.19290	0.32130
min	-0.18060	-0.23120	-0.10000
mean	0.00678	-0.01362	0.04524
std	0.07345	0.07916	0.04715

table 3

1 month	***x***	***y***	***z***
max	0.35070	0.87610	0.32130
min	-0.76970	-0.33130	-0.41410
mean	-0.00420	-0.01126	0.01743
std	0.08890	0.08117	0.05795

Figure 8 shows the differences in position over a period of one month. The three graphs represent the differences in the x, y and z coordinates. It strikes that the z component which is the most interesting one because it gives the height of the satellite seems also to be the most stable one. There are not such big extremes as occur in the x and y component. Table 1 to table 3 ascertain this observation by the fact that the z component has the lowest standard deviation during all kind of

different periods.

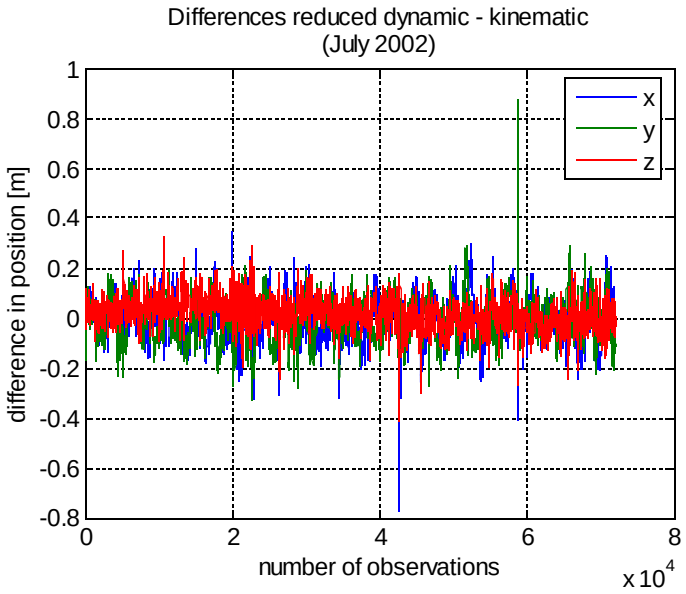

figure 8: differences in position (July 2002)

Table 4 to table 6 correspond to table 1 to table 3 and present the differences in velocity over a period of one day, one week and one month. Similar conclusions can be drawn from those tables as from the differences in position except for the fact that the quantities are much smaller. However, one has also to be aware that the unit is now m/s.

Differences in velocity [m/s] (*reduced dynamic – kinematic*)

table 4

1 day	***vx***	***vy***	***vz***
max	0.00117	0.00119	0.00123
min	-0.00084	-0.00094	-0.00153
mean	-0.121e-05	0.072e-05	-0.086e-05
std	0.1414e-03	0.1396e-03	0.2018e-03

table 5

1 week	***vx***	***vy***	***vz***
max	0.00142	0.00201	0.00234
min	-0.00202	-0.00147	-0.00160
mean	0.006e-06	-0.050e-05	-0.137e-05
std	0.1521e-03	0.1456e-03	0.2051e-03

table 6

1 month	*vx*	*yv*	*vz*
max	0.00191	0.00373	0.00234
min	-0.00235	-0.00147	-0.00202
mean	0.422e-06	0.422e-06	-0.665e-06
std	0.1547e-03	0.1550e-03	0.2087e-03

Figure 9 corresponds to figure 8 showing the differences in velocity. This time it cannot be determined which component is the most stable one as the extremes occur in x, y and z direction.

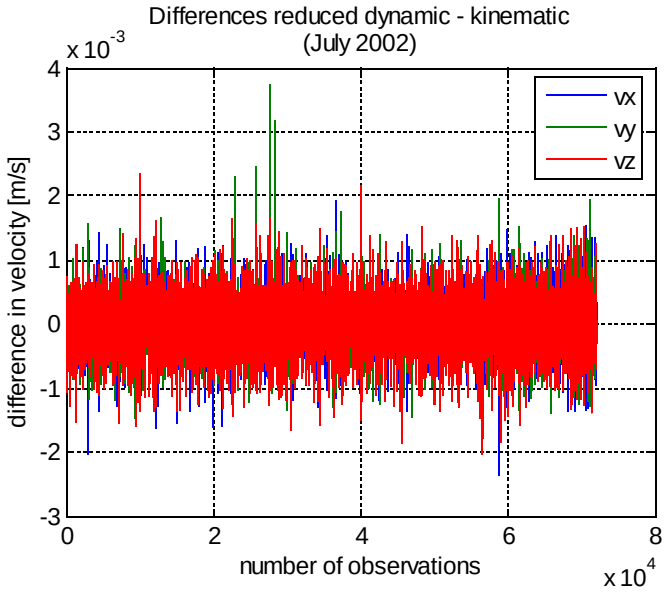

figure 9: differences in velocity (July 2002)

At this point the question arises if certain areas of the earth are more likely to show high differences in position and velocity of the two data sets than others. In order to have a closer look at the distribution of these differences, the earth is equally gridded with a spacing of 1° in North-South and East-West direction. As the grid spans over an area from -90° to +90° latitud e and from 0° to 360° longitude, 18x36 = 648 blocks are defined. The standard deviations of differences between *reduced dynamic* and *kinematic* measurements are computed per block. In contrast to the previous comparisons, the differences between *reduced dynamic* and *kinematic* are now calculated with respect to the magnitude of the position and velocity vector and not with respect to the three components in x, y

and z direction. The result of these calculations is presented in figure 10 and figure 11 which show the standard deviation of differences per block. The left plot is based on the position and the right plot on the velocity.

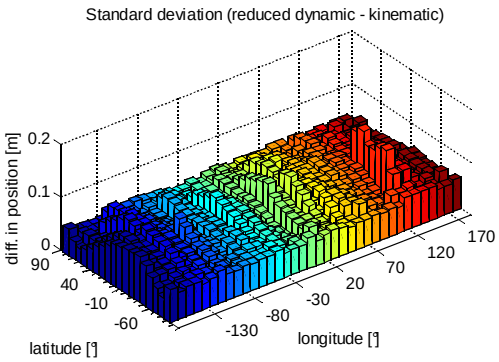

figure 10: standard deviation (position)

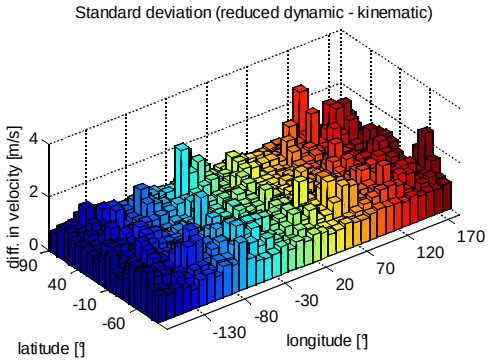

figure 11: standard deviation (velocity)

It is difficult to draw a conclusion due to those figures. A relationship between particular areas of the earth, such as mountains, and high values in differences is not obvious. It is interesting though to realize that the differences in position seem to have a North-South pattern while the standard deviations of the differences in velocity are rather arbitrarily spread. However, the reason of the observed North-South pattern has not been explained yet. Further investigations are needed to better understand the above figures.

3.5 Detection of outliers

As mentioned earlier, the advantage of two different data sets is that errors can be detected more easily. For that reason the magnitudes of the position and velocity vectors of the *reduced dynamic* and *kinematic* observations are compared. The differences are presented in figure 12 and figure 13.

The differences in position have a similar size if one refers either to the magnitudes (figure 12) or to the three x, y and z components (figure 8). The differences in velocity however are reduced by approximately a half if one considers the magnitudes (figure 13) instead of the coordinate components (figure 9).

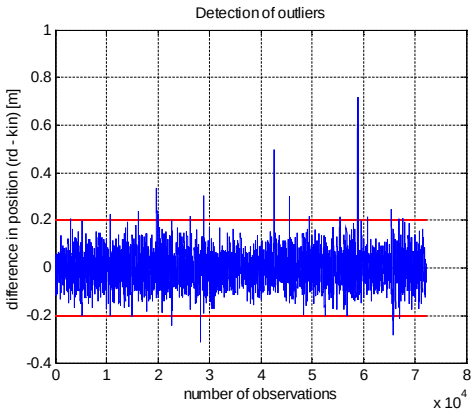

figure 12: detection of outliers (position)

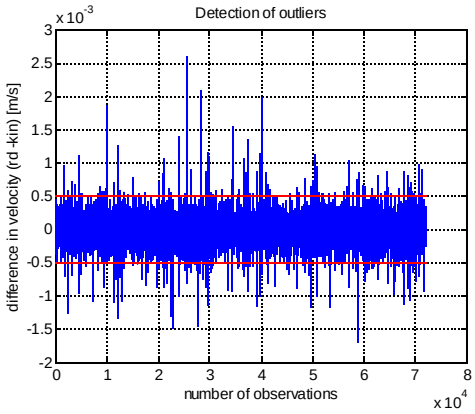

figure 13: detection of outliers (velocity)

From the above figures, the conclusion can be drawn that the majority of differences in position occur between -0.2m and +0.2m while most of the differences in velocity occur between -0.5mm/s and +0.5mm/s. Observations which lie outside these boundaries are declared outliers and deleted.

A higher difference at one point may indicate an error or a discontinuity in at least one of the two data files at that point. If those outliers are filtered, a more accurate set of data can be achieved. Around 500 out of 72,000 observations in each data set are declared outliers reducing the data sets by 0.7%.

4 Calculation of accelerations

4.1 Transformation from CTS to CIS

This chapter describes how the accelerations of the CHAMP satellite are derived from the velocities in the state vectors.

In order to achieve a reasonable value for the accelerations these should be described in an inertial reference system which is not fixed to the rotation of the earth. Otherwise the accelerations would include centrifugal and Coriolis terms as well. The satellite however is considered not to rotate with the earth and should therefore not be influenced by centrifugal forces.
Only the accelerations in an inertial system can directly be related to the earth's gravity field because Newton's law of motion is only valid in an inertial system. As a consequence the velocity vectors of the *reduced dynamic* and *kinematic* data sets have to be transformed from the Conventional Terrestrial System *CTS* to the Conventional Inertial System *CIS*. *CIS* is fixed to fundamental stars and has its origin in the centre of the mass of the earth. Since the origin undergoes small accelerations due to the annual motion of the earth around the sun, the system is called quasi-inertial.

The main difference between the space-fixed and the earth-fixed reference system can be described by a rotation around the third axis, i.e. the rotation axis of the earth, around the angle *GAST* (equation 4.1). *GAST* means Greenwich Apparent Sidereal Time and gives the time between the zero meridian at Greenwich and the true vernal equinox. *GAST* can either be expressed in seconds or in degrees.

$$\boldsymbol{R}_3(GAST) = \begin{bmatrix} \cos(GAST) & \sin(GAST) & 0 \\ -\sin(GAST) & \cos(GAST) & 0 \\ 0 & 0 & 1 \end{bmatrix} \tag{4.1}$$

As *GAST* changes according to the rotation of the earth, this angle has to be

determined for each observation of the state vector.

The first step before one can calculate *GAST* is to derive *GMST* which means Greenwich Mean Sidereal Time and defines the angle between the zero meridian at Greenwich and the mean vernal equinox. The relation between *GAST* and *GMST* is shown in figure 14.

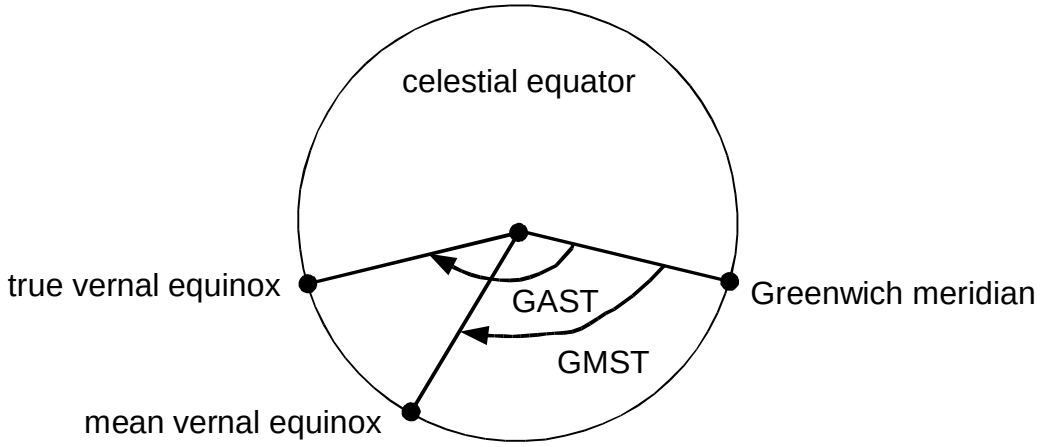

figure 14: GMST and GAST, compare [Torge 2001]

The difference in both angles is called the equation of equinoxes (equation 4.13) and is caused by the nutation and shift in the obliquity of the ecliptic.

GMST

GMST for any particular day is defined at 0h Universal Time (*UT*) by equation 4.2 [Montenbruck and Gill 2001].

$$GMST\,(0\,h\,UT) = 6^h\,41^m\,50.^s54841 + 8640184.^s812866\;T_0 + 0.^s093104\;T_0^2 - 6.^s2\,x10^{-6}\;T_0^3 \qquad (4.2)$$

$$T_0 = \frac{JD\,(0^h\,UT) - 24514545}{36525} \qquad JD: \;\; Julian\,Date \qquad (4.3)$$

The time interval T_0 (equation 4.3) contains the Julian centuries which have

elapsed since the standard epoch 2000 January 1, 12h UT, at the beginning of the day.

The definition of *GMST* (equation 4.4) for an arbitrary time of the day is given by a generalization of equation 4.2 [Montenbruck and Gill 2001].

$$\begin{aligned} GMST(UT) &= 6^h 41^m 50.^s 54841 + 8640184.^s 812866\ T_0 \\ &+ 1.^s 002737909350795\, UT + 0.^s 093104\ T_{UT}^2 - 6.^s 2\ x10^{-6}\ T_{UT}^3 \end{aligned} \tag{4.4}$$

$$T_{UT} = \frac{JD(UT) - 24514545}{36525} \qquad JD: \ Julian\ Date \tag{4.5}$$

The time interval T_{UT} (equation 4.5) is now specified by the Julian centuries that have elapsed since the standard epoch 2000 January 1, 12h UT, at the arbitrary time of the day.

As the synchronised state vectors have a time statement in Universal Time (compare Chapter 3), T_{UT} can be derived by adding the seconds of the specific day converted into Julian centuries to T_0.

GAST

Once *GMST* is known, the correction to *GAST* should be determined. This is done by a linear approximation which is valid for 50 years either side of J2000.0. The used formulas (equation 4.6 - equation 4.14) can be found on the paper “Sidereal time formulas and spreadsheet to navigation accuracy“.

(http://www.xylem.f2s.com/kepler/siderial.html)

$$\Omega = 125.04452 - 1934.136261\ T_{UT} \quad [^\circ] \tag{4.6}$$

$$L = 280.4665 + 36000.7698\ T_{UT} \quad [^\circ] \tag{4.7}$$

$$L_1 = 218.3165 + 481267.8813\ T_{UT} \quad [^\circ] \tag{4.8}$$

$$e = 23.439 - 00000004\ T_{UT} \quad [^\circ] \tag{4.9}$$

The equations above give an approximation to the following parameters:

- Ω, the longitude of the ascending node of the moon's mean orbit

- L, the mean longitude of the sun
- L_1, the mean longitude of the moon
- e, the mean obliquity of the ecliptic

In a further step $\Delta\Psi$ (equation 4.10) and $\Delta\varepsilon$ (equation 4.12) are computed where $\Delta\Psi$ being the change in the ecliptic longitude due to nutation and $\Delta\varepsilon$ being the shift in angle between the ecliptic and the equator.

$$\Delta\psi = \frac{-17.2\,\sin(\Omega) - 1.32\,\sin(2L) - 0.23\,\sin(2L_1) + 0.21\,\sin(2\Omega)}{3600} \quad [^\circ] \tag{4.10}$$

$$\Delta e = \frac{9.2\,\cos(\Omega) + 0.57\,\cos(2L) + 0.1\,\cos(2L_1) - 0.9\,\cos(2\Omega)}{3600} \quad [^\circ] \tag{4.11}$$

$$\Delta\epsilon = e + \Delta e \quad [^\circ] \tag{4.12}$$

Finally, the equation of the equinoxes (equation 4.13) is added to *GMST* as a correction (equation 4.14).

$$equation\,of\,the\,equinoxes = \Delta\psi\,\cos(\epsilon) \quad [^\circ] \tag{4.13}$$

$$GAST = GMST + equation\,of\,the\,equinoxes \quad [^\circ] \tag{4.14}$$

The above expressions are all derived in degrees.

The transformation from *CTS* to *CIS* includes in fact not just one rotation around *GAST* but a sequence of rotation matrices which account for the precision, nutation and polar motion of the earth as explained on page 14 in [Seeber 1993]. The influences of those rotation matrices are, however, considered to be very small and are therefore neglected in the following calculations.

This leads to the equation 4.15 which transforms a vector x of size 3x1 from *CTS* to *CIS*.

$$x_{CIS} = \boldsymbol{R}_3(GAST)\,x_{CTS} \tag{4.15}$$

Since in this case the vector *x* does not contain the coordinates of the position but of the velocity one has first to consider the influence of the earth's rotation on the measured velocities before the above rotation is carried out. The earth rotation terms which influence the *x* and *y* components of the velocity vector in *CTS* can be derived from equation 4.16 and 4.17 where *r* is computed by the *x* and *y* component of the position vector in *CTS*, λ is the spherical longitude of the observation and ω is the earth's angular velocity.

$$v_{ex} = -r\omega\sin(\lambda) \tag{4.16}$$

$$v_{ey} = r\omega\cos(\lambda) \tag{4.17}$$

$$with \quad r = \sqrt{x_{CTS}^2 + y_{CTS}^2} \quad \wedge \quad \omega = 7.2921151467 e^{-5} \frac{1}{s}$$

If v_{ex} and v_{ey} are added to the original values of the velocity vector, the rotation of equation 4.15 can be computed.

4.2 Newton Interpolation

4.2.1 General introduction

The idea is to change the point-wise state vectors into a continuous function through Newton Interpolation. An interpolation requires that the point-wise measurements are at these points equal to the function which approximates them. After an appropriate approximation function is found, the accelerations can be calculated by a differentiation of the continuous function.

Newton Interpolation is carried out by a polynomial of following structure (equation 4.18) where Φ being the interpolated value in *x* and *c* being the coefficients which describe the polynomial [Keller 2002]. The task is to determine the coefficients *c*.

$$\phi(x) = c_0 + c_1(x - x_0) + c_2(x - x_0)(x - x_1) + \ \ldots \ + c_n(x - x_0)\ldots(x - x_n) \tag{4.18}$$

The major advantage of Newton Interpolation in comparison to other interpolation methods is that the polynomial coefficients *c* can be easily derived from following difference scheme (table 7). This scheme requires only few numerical operations and if an interpolation point should later on be added only one more line has to be included to the scheme.

table 7

	k = 0	***k = 1***	***k = 2***	…
x_0	$\mathbf{f_0 = f[x_0]}$			
		$\mathbf{f[x_0,x_1]}$		
x_1	$f_1 = f[x_1]$		$\mathbf{f[x_0,x_1,x_2]}$	
		$f[x_1,x_2]$		…
x_2	$f_2 = f[x_2]$			
⋮	⋮	⋮	⋮	⋮

The contents of table 7 are computed by the formula of equation 4.19 and equation 4.20 [Keller 2002].

$$f\left[x_i\right] := f_i := f\left(x_i\right) \tag{4.19}$$

$$f\left[x_i, x_{i+1}, \ldots, x_{i+k}\right] := \frac{f\left[x_{i+1}, \ldots, x_{i+k}\right] - f\left[x_i, \ldots, x_{i+k-1}\right]}{x_{i+k} - x_i} \tag{4.20}$$

The polynomial coefficients *c* are now provided by the upper value of each column of table 7 which leads to table 8.

table 8

c_0	$\mathbf{f[x_0]}$
c_1	$\mathbf{f[x_0,x_1]}$
c_2	$\mathbf{f[x_0,x_1,x_2]}$
⋮	⋮

Beside the advantage of the difference scheme, Newton Interpolation also struggles with problems which generally occur with polynomial interpolations. The main problem is to determine how many interpolation points should be utilised. If there are not enough interpolation points, significant details will be missing and cannot be described. If there are on the other hand too many interpolation points, the interpolating polynomial shows a high oscillating pattern between the interpolation points, especially on the edge.
The next section will briefly discuss the different possibilities of Newton Interpolation.

4.2.2 Choice of interpolation function

Austen and Reubelt, who also worked with a CHAMP data set, tested and discussed several variations of Newton Interpolations within their thesis [Austen and Reubelt 2000]. The variations consider different amounts of interpolation points and different data that means accelerations were either derived from using positions or from using the velocities of the satellite.
A three-point, a five-point, a seven-point and a nine-point interpolation was carried out.

Austen and Reubelt found out that the seven- and the nine-point Newton Interpolation deliver the best results in the case of a low orbiting satellite with a data sampling rate of 10 to 30 seconds. They also come to the conclusion that accelerations derived from velocities are more accurate than those derived from positions as only one differentiation instead of two has to be done.

The equations of the Newton Interpolation programmed for their thesis [Austen and Reubelt 2000] are written in MATLAB and are also used within this study thesis. However, before the program is used for real data, the influence of the different MATLAB functions have been tested by using simulated data.

The simulation data are from the satellite mission GOCE (see Chapter 1) and can be downloaded from the website of the University of Bonn, Institute for Theoretical Geodesy (http://www.geod.uni-bonn.de/index.html). GOCE data are useful as they

do not only contain positions and velocities of the satellite but also the three components of the accelerations. A comparison of these accelerations and the computed accelerations allows to determine the quality of the Newton Interpolation.

The seven-point and the nine-point Newton Interpolation have both been tested with position and velocity vectors of GOCE. The results are shown below in table 9 and table 10.

Differences: interpolated accelerations – simulated accelerations [m/s^2]

table 9

	7-point (position)	***7-point (velocity)***
max	1.2192e-04	5.9209e-05
min	-2.0202e-04	-1.0098e-04
mean	1.99e-09	6.80e-10
std	1.5155e-04	7.5829e-05

table 10

	9-point (position)	***9-point (velocity)***
max	1.1849e-04	5.9266e-05
min	-2.0211e-04	-1.0102e-04
mean	1.55e-09	4.53e-10
std	1.5166e-04	7.5829e-05

The tables present the maximum, minimum, mean value and standard deviation of the differences, simulated accelerations subtracted from interpolated accelerations. The magnitudes of the acceleration vectors are compared. These results confirm Austen‘s and Reubelt‘s observation that computing accelerations from velocities is more accurate than from positions [Austen and Reubelt 2000].

The results of the nine-point and seven-point interpolation are almost of the same quality because the standard deviations of the differences are equal up to $10^{-9} m/s^2$. Since the nine-point interpolation is more complex and time-consuming than

the seven-point interpolation, only the seven-point interpolation will be used to compute the accelerations from the *reduced dynamic* and *kinematic* velocities.

4.2.3 Seven-point Newton Interpolation

Seven-point indicates, as mentioned above, that seven interpolation points are used. The most important interpolation point is the observation in the middle. Its value is interpolated by using up to three observations before and after the middle point. The interpolation formula can bee seen as a filter which is shifted over each interpolation point. Seven points are needed to calculate one acceleration.

Austen and Reubelt assume that the interpolation points are equidistant, implying that the observations have a constant sampling rate Δt. In the case of the synchronised *reduced dynamic* and *kinematic* data this sampling rate is 30s.
Bearing this in mind equation 4.18 can be simplified to equation 4.21 (compare [Austen and Reubelt 2000]). The vector $\boldsymbol{X}$ contains the velocity components in x, y, and z direction of CIS.

$$\boldsymbol{X}(t) = \boldsymbol{X}_0 + \sum_{i=1}^{n} \Delta_{i/2}^{\,i} = \boldsymbol{X}_0 + \binom{s}{1}\Delta_{1/2}^{\,1} + \binom{s}{2}\Delta_{1}^{\,2} + \binom{s}{3}\Delta_{3/2}^{\,3} + \cdots + \binom{s}{n}\Delta_{n/2}^{\,n} \qquad (4.21)$$

$$with \quad s = \frac{t}{\Delta t}$$

The parameter *s* will always be constant because of the constant sampling rate. In case of the seven-point interpolation *s* equals three while *t* represents the time.
The vector $\boldsymbol{\Delta}$ includes the differences of the velocity vectors $\boldsymbol{X}$ according to the difference scheme of equidistant observations.
These differences $\boldsymbol{\Delta}$ are obtained from the general equation 4.22 and in case of the seven-point Newton Interpolation they look like equation 4.23 [Austen and Reubelt 2000].

$$\Delta_{n/2}^{\,n} = \sum_{i=0}^{n} (-1)^{n+1} \binom{n}{i} \boldsymbol{X}_i \qquad (4.22)$$

$$
\begin{aligned}
\Delta^{1}_{1/2} &= \boldsymbol{X}_1 - \boldsymbol{X}_0 \\
\Delta^{2}_{1} &= \boldsymbol{X}_2 - 2\boldsymbol{X}_1 + \boldsymbol{X}_0 \\
\Delta^{3}_{3/2} &= \boldsymbol{X}_3 - 3\boldsymbol{X}_2 + 3\boldsymbol{X}_1 - \boldsymbol{X}_0 \\
\Delta^{4}_{2} &= \boldsymbol{X}_4 - 4\boldsymbol{X}_3 + 6\boldsymbol{X}_2 - 4\boldsymbol{X}_1 + \boldsymbol{X}_0 \\
\Delta^{5}_{5/2} &= \boldsymbol{X}_5 - 5\boldsymbol{X}_4 + 10\boldsymbol{X}_3 - 10\boldsymbol{X}_2 + 5\boldsymbol{X}_1 - \boldsymbol{X}_0 \\
\Delta^{6}_{3} &= \boldsymbol{X}_6 - 6\boldsymbol{X}_5 + 15\boldsymbol{X}_4 - 20\boldsymbol{X}_3 + 15\boldsymbol{X}_2 - 6\boldsymbol{X}_1 + \boldsymbol{X}_0
\end{aligned}
\tag{4.23}
$$

Equation 4.21 defines a function which calculates an interpolated velocity vector at any given time. The first derivative of this function with respect to time gives an acceleration vector at any time (equation 4.24). Only *s* depends on time.

$$
\begin{aligned}
\dot{\boldsymbol{X}}(t) &= \binom{s}{1}' \Delta_{1/2}{}^{1} + \binom{s}{2}' \Delta_{1}{}^{2} + \binom{s}{3}' \Delta_{3/2}{}^{3} + \cdots + \binom{s}{n}' \Delta_{n/2}{}^{n} \\
&= \frac{1}{\Delta t}\left\{ \Delta^{1}_{1/2} + \frac{2s-1}{2!}\Delta^{2}_{1} + \frac{3s^2-6s+2}{3!}\Delta^{3}_{3/2} + \cdots + \frac{1}{n!}\sum_{k=0}^{n-1}\frac{\prod_{i=0}^{n-1}(s-i)}{s-k}\Delta^{n}_{n/2} \right\}
\end{aligned}
\tag{4.24}
$$

$\dot{\boldsymbol{X}}(t)$ are finally the acceleration vectors which are needed for the computations of the gravity field (Chapter 5). If the input data ***X***, however, were not velocities but positions then the accelerations would be given by the second derivative of the polynomial function (equation 4.21), that means $\ddot{\boldsymbol{X}}(t)$ would have to be calculated. Since the second derivative causes some additional inaccuracies (compare previous section 4.22) only velocities are utilised as input data.

4.2.4 Application to *reduced dynamic* and *kinematic* data sets

Due to the fact that CHAMP data are not continuous and that even more gaps occur after data preprocessing (Chapter 3), the *reduced dynamic* and *kinematic* data sets have to be divided into blocks of equidistant observations. If the time to a following observation lasts longer than 30s, a new block will be created starting with this following observation.

Seven-point Newton Interpolation is carried out for each velocity vector except for

the velocities on the edge of a block. Since seven interpolation points are needed per observation, no interpolation can be calculated for the first and last three observations of a block. These edge observations are omitted so that the *reduced dynamic* and *kinematic* data files only consist of state vectors wich have corresponding accelerations.

4.3 Comparison to reference model

After the accelerations were derived from the *reduced dynamic* and *kinematic* velocities, it is interesting to find out how well they fit to a reference model. The Earth Gravity Model 96 (EGM96), is chosen as reference model [Lemoine et al. 1998]. EGM96 is a gravity model which exists of spherical harmonic coefficients up to a degree and order of 360.

The *reduced dynamic* and *kinematic* magnitudes of accelerations are subtracted from those accelerations which are derived from EGM96. The maximum, minimum, mean and standard deviation of the differences that occur within July 2002 are shown in table 11 (*reduced dynamic*) and table 12 (*kinematic*).

table 11

Differences in acceleration [m/s^2] (EGM96 – reduced dynamic)

max	***min***	***mean***	***std***
2.589e-05	-1.632e-05	-7.144e-08	3.169e-06

table 12

Differences in acceleration [m/s^2] (EGM96 – kinematic)

max	***min***	***mean***	***std***
8.368e-05	-8.933e-05	-8.077e-08	1.038e-05

The majority of the differences in both cases are of size 10^{-5}m/s^2, i.e. around a few mgals. The *reduced dynamic* accelerations are more consistent to EGM96 than the *kinematic* although *reduced dynamic* and *kinematic* differences have similar sizes. This is supported by the differences in standard deviations (0.3mgal versus 1mgal) which emphasizes that the *reduced dynamic* data are slightly more accurate than the *kinematic*.

The above calculated differences are plotted in figure 15. Here the same conclusions are drawn as before. The *reduced dynamic* accelerations (red) show smaller amplitudes, that means these accelerations have less differences to EGM96 than the *kinematic* accelerations (blue).

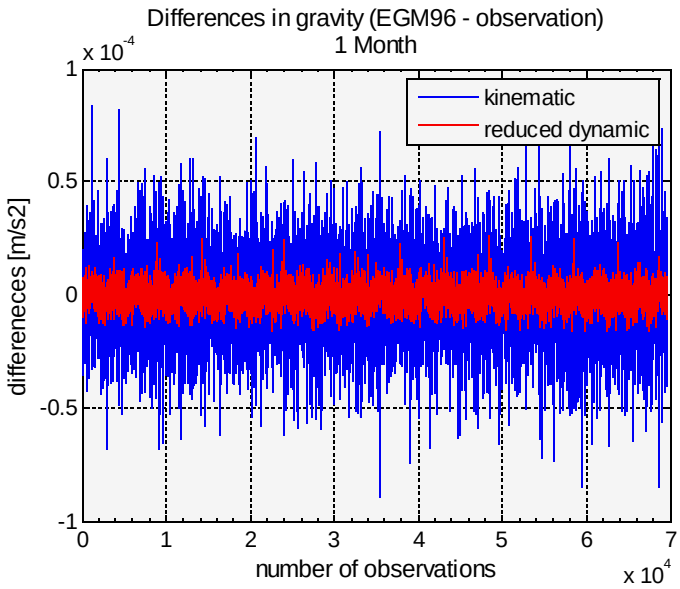

figure 15: differences in gravity

The main problem of the *kinematic* data is probably that the GPS measurements cause too much noise. As a result, an orbit described by the *reduced dynamic* data becomes smoother than the *kinematic* orbit.
Nevertheless, both data sets are used to derive a gravity field model.

Another conclusion drawn from figure 15 is that the differences show a kind of an oscillating pattern. This could be caused by additional accelerations which cannot directly be derived from the earth‘s gravity field. These accelerations are also called perturbing accelerations. Possible improvements of this problem are discussed in section 4.4 and 4.5.

4.4 Correction due to tide

The accelerations so far are influenced by tidal accelerations and should therefore be corrected.

Tidal accelerations are caused by the superposition of lunisolar gravitation and

orbital accelerations due to the motion of the earth around the barycentre of the respective two-body system [Torge 2001]. The gravitational impact of other planets is usually neglected as it is too small. One considers the moon due to its close distance to the earth and the sun due to its enormous size.

The earth's gravity field is symmetrically deformed by these tidal effects which are both time- and latitude-dependent. The tidal correction is greatest at low latitudes and has a strong periodic component with period on the order of 12 hours [Blakely 1996] due to the rotation of the earth about its axis.

Formulas exist [Longman 1959] which calculate the tidal correction for any point on the earth at any time. The same formulas are now used to calculate the tidal effect on the satellite. That means the point of interest does not lie on the surface of the earth but in the satellite. This change however does not alter the formulas that are utilised.

table 13

Tidal correction in m/s^2

max	***min***	***mean***	***std***
1.797e-06	-9.311e-07	-1.545e-07	5.878e-07

Table 13 shows the result of the tidal corrections which should be applied to the *reduced dynamic* and *kinematic* data sets. As shown in the table above, the maximum, minimum and mean value of the tidal corrections as well as the standard deviation are in the range of $10^{-7} m/s^2$. These values are too small to show a significant improvement to the accelerations. Regarding table 11 and table 12, it can be stated that 10^{-7} is a size which lies within the noise of the data. For that reason the tidal accelerations are not considered in the following process.

4.5 Correction due to non-gravitational forces

Non-gravitational forces acting on the satellite are responsible for the non-gravitational accelerations. As previously mentioned in Chapter 2, accelerometers are placed on board of CHAMP in order to measure those non-gravitational

accelerations.
The two main causes which effect these accelerations are the atmospheric drag and the solar radiation pressure.

Atmospheric forces are the largest non-gravitational perturbations which act on low orbiting satellites such as CHAMP. These forces are caused by the interaction of the satellite with particles in the atmosphere and depend on following elements [Seeber 1993]:

- geometry of the satellite
- velocity of the satellite
- orientation of the satellite with respect to the flow
- density, temperature and composition of the atmospheric gas.

The disturbing forces are biggest when the satellite is close to the earth during daytime.

Solar radiation pressure on a satellite results from the absorption or reflection of photons that are continuously emitted by the sun. The magnitude of the force depends on [Montenbruck and Gill 2001]:

- effective satellite surface area
- reflectivity of satellite surface
- solar flux
- distance between satellite and sun

The magnitudes of non-gravitational accelerations which occurred in July 2002 were derived and their maximum, minimum, mean value and standard deviation calculated (table 14).

table 14

Non-gravitational accelerations in m/s^2

max	***min***	***mean***	***std***
1.736e-06	0	3.887e-07	1.431e-07

The non-gravitational accelerations in table 14 have similar quantities than the

tidal corrections in table 13 with the specification that they are all positive as they only decelerate the satellite.

From that, one can conclude that non-gravitational accelerations are also too small to be taken into account within this study. Again corrections lie within the range of noise of data and are therefore rejected in the following processes.

5 Calculation of spherical harmonic coefficients

5.1 Theory of Least-Squares Collocation

The aim of this Chapter is to describe the prediction of spherical harmonic coefficients using Least-Squares Collocation. The method of collocation was first derived around the 1970s. Its original task was to determine the anomalous gravity field using geodetic measurements of arbitrary quantities, which must however be related to the anomalous potential. The anomalous potential *T* is of special interest as it may be represented by a series which contains the spherical harmonic coefficients.

First of all, one can present *T* in equation 5.1 where *λ,φ,r* are again the spherical coordinates of an arbitrary point *P*, with *G* being the universal gravitational constant, *M* the earth's mass and *a* the semi-major axis of the reference ellipsoid. A spherical approximation is used throughout the following calculations although the equations refer to *a.*

Due to the fact that *T(P)* is a square integrable and harmonic function it can be expanded into a series of surface spherical harmonics (equation 5.1) where $\bar{P}_{ij}(\sin(\varphi_p))$ are the fully normalized Legendre functions of the first kind. These functions multiplied by sine or cosine of the longitude are the surface spherical harmonics (equation 5.2). The development of the anomalous potential starts at *i* = 2 because it is assumed that the masses of the earth and the reference sphere are equal, and that the centre of the earth's masses coincides with the centre of the reference sphere.

$$T(P) = T(\lambda_p, \varphi_p, r_p) \tag{5.1}$$

$$= \frac{GM}{r_p} \sum_{i=2}^{\infty} \left(\frac{a}{r_p}\right)^i \sum_{j=-i}^{i} \bar{P}_{ij}(\sin(\varphi_p)) \begin{cases} \cos(j\lambda_p)\, c_{ij} & if \quad j \geq 0 \\ \sin(j\lambda_p)\, s_{ij} & if \quad j < 0 \end{cases}$$

$$V_{ij}(\lambda,\varphi) = \bar{P}_{ij}(\sin(\varphi))\begin{Bmatrix}\cos(j\lambda)\\ \sin(j\lambda)\end{Bmatrix}\quad\begin{matrix} if & j\geq 0\\ if & j<0\end{matrix} \tag{5.2}$$

This series development (equation 5.1) is only correct outside a sphere bounding all masses. However, it has been shown (Runge theorem) that T may be approximated everywhere outside a sphere which is enclosed in the earth by a similar series development. The summation of that series development goes up to some degree N depending on how well the anomalous potential should be approximated.

The equation of the anomalous potential can be rearranged into an equation of the spherical harmonic coefficients c_{ij} and s_{ij} (equation 5.3).

$$\frac{GM}{a}\begin{Bmatrix}c_{ij}\\ s_{ij}\end{Bmatrix} \tag{5.3}$$

$$= \frac{1}{4\pi}\int_{\varphi=-\frac{\pi}{2}}^{\frac{\pi}{2}}\int_{\lambda=0}^{2\pi}\bar{P}_{ij}(\sin(\varphi_p))\,T(P)\begin{Bmatrix}\cos(j\lambda_p)\\ \sin(j\lambda_p)\end{Bmatrix}\cos(\varphi_p)\,d\lambda\,d\varphi\quad\begin{matrix} if & j\geq 0\\ if & j<0\end{matrix}$$

In order to calculate the spherical harmonic coefficients either *T(P)* must be given as for example mean or point value in a grid or an approximation to *T(P)* has to be found. In this case the task is to find an approximation. This can be achieved by Least-Squares Collocation which in general looks for the best estimation of *T(P)* on the basis of the measured data *l*. Best estimation means that the squares of the differences between the observations and the model *T(P)* have to be minimized. The connection between *T(P)* and the data *l* is thereby expressed in terms of covariance matrices. Equation 5.4 illustrates this relationship in matrix notation [Moritz 1980].

$$\hat{T}(P) = \begin{bmatrix} C_{p1} & C_{p2} & \cdots & C_{pN} \end{bmatrix} \begin{bmatrix} C_{11} & C_{12} & \cdots & C_{1N} \\ C_{21} & C_{22} & \cdots & C_{2N} \\ \vdots & \vdots & & \vdots \\ C_{N1} & C_{N2} & \cdots & C_{NN} \end{bmatrix}^{-1} \begin{bmatrix} l_1 \\ l_2 \\ \vdots \\ l_N \end{bmatrix} \tag{5.4}$$

The anomalous potential *T* in a point *P* equals the products of the covariance vector C_{pi} between *P* and the measured quantities, of the inverse cross-covariance matrix C_{ij} between each measurement and of the vector *l* which holds the values of the measurements. The inverse of the so-called normal equation matrix C_{ij} exists as all covariance matrices are positive definit and have therefore full rank. This requires that no observation occurs more than once which implies linear independence. The index *N* stands for the number of measurements.

The same expression (equation 5.4) can also be written as a series (equation 5.5) in a slightly different notation [Tscherning 2001].
The elements b_k are the solutions of the normal equations and are constant.

$$\begin{aligned} \hat{T}(P) &= \sum_{k=1}^{N} b_k \, cov(T(P), obs_k) \\ with \quad \{b_i\} &= \{cov(i,j)\}^{-1} \{obs_j\} \end{aligned} \tag{5.5}$$

The abbreviation *obs* stands for observation. Within this study the observations are chosen to be the gravity disturbance *δg* because of their simple relation to the anomalous potential *T*. Furthermore, *δg* are invariant under rotation of the coordinate system. The input (equation 5.6) of the following computations are the normal gravities γ subtracted from the magnitudes of the accelerations *accel* or gravities *g* which are derived as explained in the previous Chapter 4.

$$\delta g = \|accel\| - \gamma \qquad with \quad \|accel\| = g \tag{5.6}$$

At this point it should be reminded that a spherical approximation is used.

The question arises through which function the covariances should be obtained.

Equation 5.7 defines the covariance function of the anomalous potential *T* in two different arbitrary points, *P* and *Q*, by a spherical harmonic expansion [Tscherning 2001]. This is considered as the basic covariance function.

$$cov(T(P),T(Q)) \;=\; \sum_{i=2}^{\infty} \sigma_i^2 \left(\frac{R_B^2}{r_p\, r_k} \right)^{i+1} P_i(\cos(\psi))_{p,k} \tag{5.7}$$

However, as shown in equation 5.5 a covariance function is needed which describes the covariances between *T* and the observations *obs*. This demanded function can easily be derived by multiplying one more factor to the basic function since the observations consist of gravity disturbances (equation 5.8). Compare equation 2.12 or 5.6.

$$cov(T(P),obs_k) \;=\; \sum_{i=2}^{\infty} \sigma_i^2 \;\frac{i+1}{r_k}\; \left(\frac{R_B^2}{r_p\, r_k} \right)^{i+1} P_i(\cos(\psi))_{p,k} \tag{5.8}$$

The radius R_B is the so-called Bjerhammar sphere. The so-called degree variances are represented by σ_i^2 which are calculated by using fully normalized harmonic coefficients that are here a priori known from the EGM96 (equation 5.9) [Moritz 1980].

$$\sigma_i^2 \;=\; \left(\frac{GM}{a} \right)^2 \sum_{j=0}^{i} \left[\bar{c}_{ij}^{\;2} + \bar{s}_{ij}^{\;2} \right] \tag{5.9}$$

P_i are the usual Legendre polynomials which only depend on the spherical distance, namely the angle ψ between two radius vectors. The indices *p* and *k* signify that these two radius vectors belong to a point *P* where *T* should be predicted and to a point *K* where the observation obs_k takes place. This is demonstrated by figure 16.

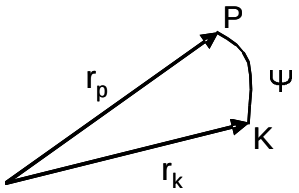

figure 16: spherical distance

As stated above, the usual Legendre polynomials can also be expressed by surface spherical harmonics (equation 5.2). Equation 5.10 shows the relationship between the Legendre polynomials and the surface spherical harmonic functions which depend on the spherical coordinates λ and φ of the point *P* as well as of the observation obs_k. This equation is called the decomposition formula or addition theorem for spherical harmonics [Moritz 1980].

$$P_i(\cos\psi)_{p,k} = \frac{1}{2i+1} \sum_{j=-i}^{i} V_{ij}(\lambda_p, \varphi_p)\, V_{ij}(\lambda_k, \varphi_k) \tag{5.10}$$

Now that an approximation for the anomalous potential has been found this solution can be substituted into equation 5.3. The result of this substitution is shown below (equation 5.11).

$$\frac{GM}{a} c_{ij} = \sum_{k=1}^{N} b_k \frac{1}{4\pi} \iint_{\sigma} cov(T(P), obs_k)\, V_{ij}(\lambda_p, \varphi_p)\, d\sigma \tag{5.11}$$

The subscript sigma at the integral sign indicates that the integral is extended over the whole unit sphere with respect to equation 5.12 [Heiskanen and Moritz 1996].

$$\iint_{\sigma} (\circ)\, d\sigma = \iint_{\varphi,\lambda} (\circ) \cos(\varphi)\, d\lambda\, d\varphi \tag{5.12}$$

If the covariance function is substituted as well, the equations of the spherical harmonic coefficients will have the form as shown in equation 5.13.

$$\frac{GM}{a} c_{ij} = \sum_{k=1}^{N} b_k \sigma_i^2 \frac{i+1}{r_k} \left(\frac{R_B^2}{a r_k} \right)^{i+1} \frac{1}{2i+1} V_{ij}(\lambda_k, \varphi_k) \tag{5.13}$$

The double integral and the spherical harmonics of the point P dissolve due to the orthogonality relation of the surface spherical harmonics. This means that the integral over a product of two equal normalized spherical harmonics is 4π (equation 5.14) [Heiskanen and Moritz 1996].

$$\frac{1}{4\pi} \iint_{\sigma} V_{ij}(\lambda, \varphi)^2 \, d\sigma = 1 \tag{5.14}$$

The radius r_p of the point *P* is set to *a* which is defined by the semi-major axis of the reference ellipsoid. If one prefers to calculate the spherical harmonic coefficients referring to the Bjerhammar sphere instead, r_p will be of the same quantity as R_B and will therefore be crossed out.
Only the elements which depend on the observations obs_k such as b_k and λ_k, φ_k, r_k influence the spherical harmonic coefficients. Since all observations are known these elements are constants. At this point it is possible to compute the coefficients of the earth's gravity field.

As yet however, it has not been considered that the observations, namely the gravity disturbances, are influenced by noise. In order to take this fact into account the variance-covariance matrix *D* should be added to the normal-equation matrix C_{ij}. Equation 5.4 is altered to the form as shown by equation 5.15 [Moritz 1980].

$$\hat{T}(P) = \begin{bmatrix} C_{p1} & C_{p2} & \cdots & C_{pN} \end{bmatrix} \begin{bmatrix} C_{11}+D_{11} & C_{12}+D_{12} & \cdots & C_{1N}+D_{1N} \\ C_{21}+D_{21} & C_{22}+D_{22} & \cdots & C_{2N}+D_{2N} \\ \vdots & \vdots & & \vdots \\ C_{N1}+D_{N1} & C_{N2}+D_{N2} & \cdots & C_{NN}+D_{NN} \end{bmatrix}^{-1} \begin{bmatrix} l_1 \\ l_2 \\ \vdots \\ l_N \end{bmatrix} \tag{5.15}$$

The matrix *D* is a variance-covariance matrix of the same form as would be used in an ordinary Least-Squares Adjustment.

If all observed data are uncorrelated and have the same variances, which is assumed for the gravity disturbances, then *D* will be reduced to a diagonal matrix with a constant factor *n* (equation 5.16).

$$\boldsymbol{D}_{nn} = \begin{bmatrix} n^2 & & 0 \\ & \ddots & \\ 0 & & n^2 \end{bmatrix} \tag{5.16}$$

Finally, the error estimation can be evaluated by equation 5.17 where C_0 is the autocovariance of the predicted anomalous potential *T,* and *E* are the standard errors of the prediction.

$$\boldsymbol{E}^2 = \boldsymbol{C}_0 - \{cov(T(P), obs_k)\}^T \{cov(i, j)\}^{-1} \{cov(T(P), obs_k)\} \tag{5.17}$$

5.2 Reducing data

After processing the steps in Chapter 3 and 4 the number of observations has been reduced from approximately around 86000 down to 70000. However, if the collocation steps are computed with all these observations it will still be a very time-consuming process especially when solving the normal equations which would become a large system of equations. For that reason it has been decided to thin out the data set and to reduce its amount down to one third of it.

The simplest procedure to achieve this reduction is to take every third observation and to delete the others. The total number of observations is then 23200.

In a second set-up the idea comes to account that those orbits which are close to another orbit should be deleted as they hardly deliver any new information. By using this method it might be achieved to get an equal distribution of data over the earth.
In order to realize this, the observations are divided into 403 revolutions while each revolution lasts for 93.55min which is the average time of a CHAMP satellite revolution (see Chapter 2).

It is tried to judge the similarity of two revolutions by looking on their distance on the equator. If the latitudes of two revolutions are zero similar longitudes will indicate that these two orbits are close to each other (figure 17). Assuming that the size of the orbits for each revolution are almost the same.

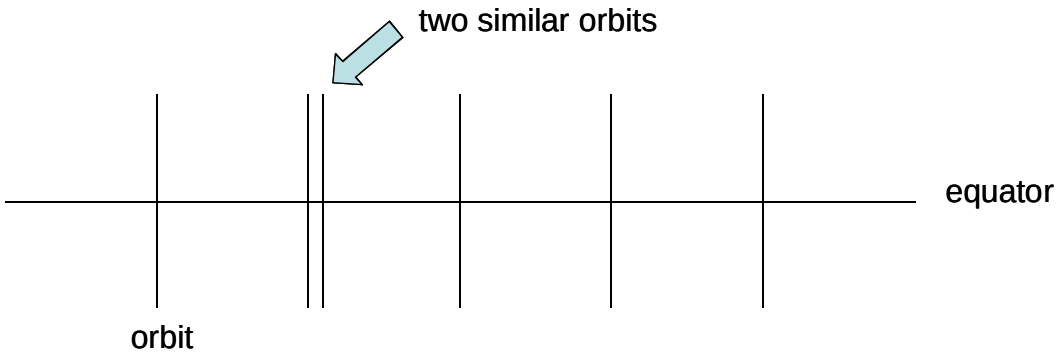

figure 17: satellite tracks at equator

As the revolution is not given in a continuous form but only by the observed points, the latitude will unlikely become exactly 0°. For that an interval along the equator of ±1° is defined. The latitude which lies within t hese borders is found for each revolution. However, 5% of the revolutions do not have an observation point close to the equator and are therefore deleted in advance. The corresponding longitudes to the selected latitudes are then compared to each other. If the difference in longitude of two orbits are within the interval of ±2° only one of the orbits will be kept for later calculations. Finally, 28% of the 403 revolutions are selected.

The result of the two methods, taking every third observation and comparing the orbits, can be seen on the two following maps (figure 18 and figure 19) created with GMT [Wessel and Smith 1998]. The source file of the GMT program is enclosed in appendix A.

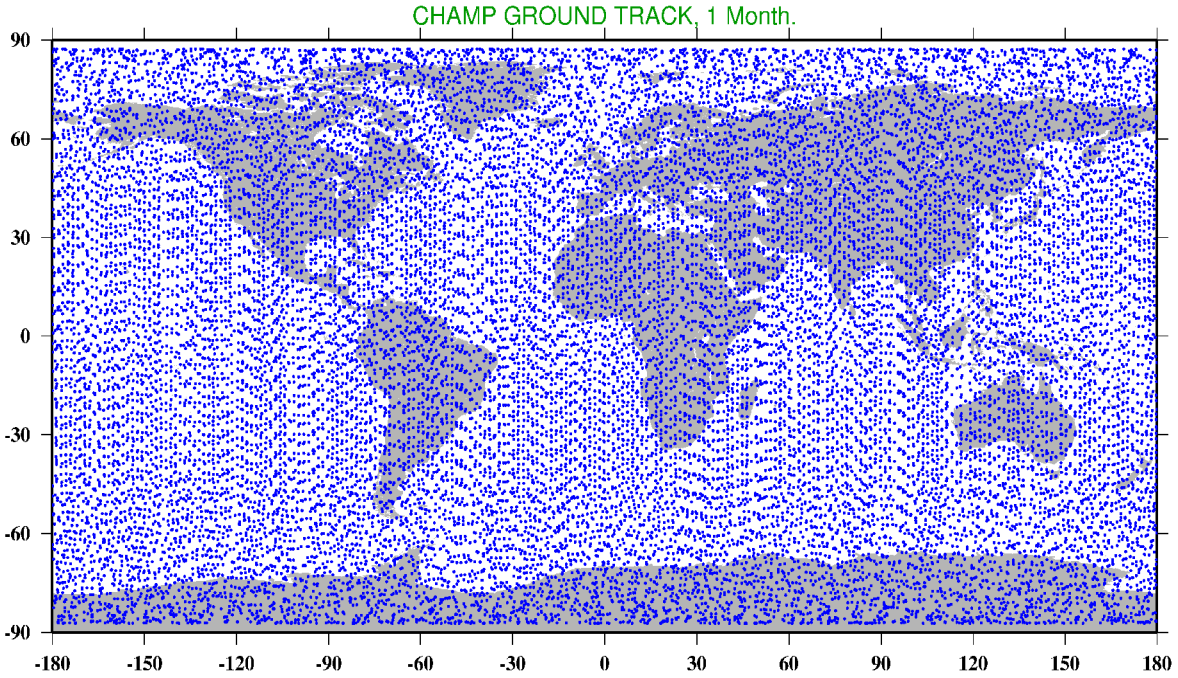

figure 18: ground tracks (method one)

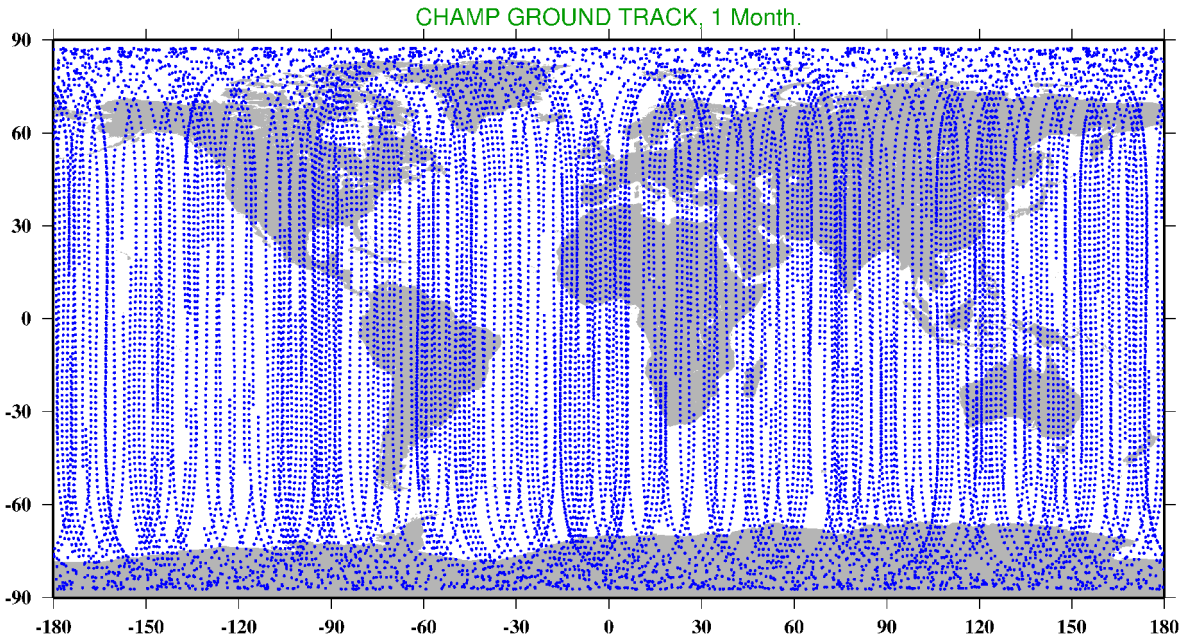

figure 19: ground tracks (method two)

Both figures present the distribution of the selected data sets. Each observation is illustrated as a small blue circle on the map. Surprisingly, several data gaps occur in the map of the second method (figure 19) while the first map (figure 18) shows an equally spread distribution of observations over the whole map, except for the polar regions.

Two of the major problems of the second method are probably that the compared longitudes are not exactly located on the equator but only within the defined borders. This leads to inaccuracies. Secondly, several gaps appear in the observations so that some orbits are deleted although they are the only data in certain areas.

It can be concluded that comparing the revolutions only at the equator is a weak method to filter useful data. However, as the results of the first method are satisfying enough, no more considerations are put into this process. Further work will only utilise data reduced by the first method.

5.3 GRAVSOFT program GEOCOL

The program which computes the Least-Squares Collocation is the GRAVSOFT [Tscherning et al. 1994] program GEOCOL [Tscherning 1974]. It is written in FORTRAN and is based on the formulas presented above (section 5.1). As GEOCOL is designed to solve many different applications, concerning for example the data types in the input and output files, the user has to set several parameters with boolean or qualitative values to get the demanded results. These user-defined parameters can be filled into a so-called job-file. The job-file which was used for this work is given in appendix B.
A detailed description of GEOCOL and its parameters can be found on the website http://www.gfy.ku.dk/~cct/geocol16v2.html.

5.3.1 Input and output

In this case the input file of GEOCOL contains five columns for the 23200 observations. The first column holds a sequence number such as the seconds of the month, the second to the fourth column are filled with the x, y and z components of the position vector of the satellite given in CTS and finally the fifth column contains the observations, namely the gravity which is later on converted into gravity disturbances within GEOCOL utilising equation 2.12.

The output file of the program contains a list and description of the parameters

which have been predefined by the user and several values which result from different computation steps. The last part of the output consists of the spherical harmonic coefficients sorted by their degree and order. Appendix B shows an output file in order to give more details about its contents and structure. At some points this file has been shortened in contrary to the original one.

5.3.2 Remove-restore

The created job-file for this work causes that a remove-restore procedure takes place within GEOCOL. Remove-restore means that a known gravity field model, in this case EGM96, is subtracted from the observed data before the calculations start and is later on added again to the results. The low degree coefficients of the earth‘s gravity field are supposed to be well known and are therefore not necessary to be calculated. Due to that the gravity disturbances based on EGM96 up to a degree and order of 24 are subtracted from the observed gravity disturbances. The differences rather than the full values are then used as observations obs_k.

This has the positive effect that only the improvements of the set of coefficients up to degree and order 24 and not their total values need to be determined. Another advantage is that using the differences instead of the full values results in a better and more uniform signal-to-noise ratio which is important for the filtering within the Least-Squares Collocation. Another important purpose is to statistically homogenize the data which means that the variances of the observations become smaller. This leads to an improvement of the linearisation during collocation.
The spherical harmonic coefficients in the output file do therefore not contain the observed EGM96 components up to degree and order 24. These observed coefficients need to be added again in order to complete the resulting set of coefficients
24 has proved to be a reasonable number for the a priori gravity field but this as well as the model itself can be changed to any other in the job-file.

5.3.3 Error propagation

One more comment should be made on the equation of the covariances 5.8. This

expression can only be used if all degree variances are known. As mentioned above, the degree variances can be computed from EGM96. However, this is only reasonable up to degree 24. EGM96 is not accurate enough to calculate degree variances of higher degree than 24. For that reason covariance propagation is used. This means that equation 5.8 is split into two series where the first part consists of known degree variances up to degree 24 while the second part uses a model for the degree variances (equation 5.18).

$$\begin{aligned} cov(T(P), obs_k) \;=\; & a \sum_{i=2}^{24} \sigma_i^2 \;\; \frac{i+1}{r_k} \;\; \left(\frac{R_B^2}{r_p \, r_k} \right)^{i+1} P_i(\cos(\psi))_{p,k} \\ & + \sum_{i=25}^{\infty} \frac{A}{(i-1)(i-2)(i+4)} \;\; \frac{i+1}{r_k} \;\; \left(\frac{R_B^2}{r_p \, r_k} \right)^{i+1} P_i(\cos(\psi))_{p,k} \end{aligned} \tag{5.18}$$

In order to solve equation 5.18 the parameters *a*, R_B and *A* have to be determined within GEOCOL. While the constant factor *a* is directly known, R_B and *A* are indirectly given as $R\text{-}R_B$ and as $cov(\Delta g_p, \Delta g_p)$. The three values of *a*, $R\text{-}R_B$ and $cov(\Delta g_p, \Delta g_p)$ must be entered into the job-file of GEOCOL.
$R\text{-}R_B$ presents the depth of the Bjerhammar sphere. As the radius of the earth is known it is possible to calculate the radius of the Bjerhammar sphere R_B.

As demonstrated by equation 5.19, $cov(\Delta g_p, \Delta g_p)$ defines the covariance of gravity anomalies. The value of *A* is calculated so that equation 5.19 becomes true for a certain value of $cov(\Delta g_p, \Delta g_p)$.

$$\begin{aligned} cov(\Delta g_p, \Delta g_p) \;=\; & a \sum_{i=2}^{24} \sigma_i^2 \;\; \frac{(i-1)^2}{r_k^2} \;\; \left(\frac{R_B^2}{r_p \, r_k} \right)^{i+1} P_i(\cos(\psi))_{p,k} \\ & + \sum_{i=25}^{\infty} \frac{A}{(i-1)(i-2)(i+4)} \;\; \frac{(i-1)^2}{r_k^2} \;\; \left(\frac{R_B^2}{r_p \, r_k} \right)^{i+1} P_i(\cos(\psi))_{p,k} \end{aligned} \tag{5.19}$$

The three input values for the job-file of GEOCOL which were used within this study are listed in table 15. They had been determined by a Fortran program called COVFIT [Knudsen 1987]. This program is based on the iterative fitting of

covariances by a curvature.

table 15

a	1.03
R-R$_B$	1.561 km
cov(Δg$_p$,Δg$_p$)	540.9 mgal^2

5.3.4 Error estimation

The influence of noise should also be considered as explained in section 5.2. For that reason the constant factor *n* of the error variance-covariance matrix (equation 5.16) is set equal to the common standard deviation of the observations. This standard deviation is chosen to be 0.3mgal in case of the *reduced dynamic* data and to be 1.0mgal in case of the *kinematic* data. These numbers are taken from the standard deviations obtained by a comparison of EGM96 in table 11 and 12 which give an approximation for the correct values. To be more correct the standard deviation of the accelerations should have been calculated by an error propagation with respect to the standard deviation of the velocities which is known.

After the coefficients are computed an error estimation is carried out. Since the error estimation of the spherical harmonic coefficients are more interesting than the errors of the anomalous potential itself, equation 5.17 is converted into equation 5.20. C_0 are now the autocovariances of GM/ac_{ij}.

$$\boldsymbol{E}^2 = \boldsymbol{C_0} - \{cov(\frac{GM}{a}c_{ij}, obs_k)\}^T \{cov(i,j)\}^{-1} \{cov(\frac{GM}{a}c_{ij}, obs_k)\} \qquad (5.20)$$

During the calculations of the coefficients the *N* solutions of the normal equations system b_k (equation 5.5) and the Cholesky decomposition of the inverse of the normal-equation matrix C_{ij} are stored in several binary files which can be used for later computations. The following computation of the covariances between the coefficients and the observations obs_k is fastened up due to the advantage that the stored Cholesky reduced matrix can be reused.

E finally gives the errors of the predicted spherical harmonic coefficients.

In order to carry out the error estimation the original job-file has to be slightly altered. The new job-file is also included in appendix B.

6 Energy Conservation

The energy conservation method has been carried out within earlier projects [Howe et al. 2003] to estimate a gravity field model. As that model will later be compared to the results of this work it is worth to give a short introduction of the idea of the method.

The energy conservation method uses the state vector of the satellite as well as measurements of non-gravitational forces to determine the gravitational potential of the earth.

The gravitational potential can be expressed by equation 6.1 as the kinetic energy of the satellite $\frac{1}{2}v^2$ minus the loss of energy [Howe et al. 2003].

$$V = \frac{1}{2}v^2 - V_{sun} - V_{moon} - \omega\left(xv_y - yv_x\right) - F - E_0 - U \tag{6.1}$$

V_{sun} and V_{moon} are the tidal potentials of the sun and moon corresponding to a rigid earth [Longman 1959]. The potential rotation term $\omega(xv_y\text{-}yv_x)$ considers the rotation of the earth's potential in an inertial frame [Jekeli 1999]. F accounts for the non-gravitational forces and E_0 stands for an integration constant. The last term U is the earth's normal potential without the centrifugal term.

Based on the results of the energy conservation method a Fast Spherical Collocation has finally estimated the spherical harmonic coefficients [Sansó and Tscherning 2003].

7 Results

This Chapter is divided into two parts. The first part has a close look at the derived gravity disturbances while the second part deals with the spherical harmonic coefficients that result from collocation. These coefficients are also compared to the coefficients derived from the energy conservation method.

7.1 Gravity disturbances

Reduced dynamic and *kinematic* accelerations create the input of GEOCOL and are calculated to gravity disturbances within that program (compare section 5.1). These gravity disturbances are declared as observations.
The gravity disturbances which are derived from EGM96 are on the other hand referred to as predictions.

The differences between predictions and observations are given in the output file of GEOCOL (appendix C). Due to them it is possible to understand the distribution of these data that are treated as input observations for the collocation. It is important to make sure that the data are normal distributed since this is desired for the concluding error estimation (equation 5.20). Data that follow a normal distribution allow a usual interpretation of the error estimation.

The following figure 20 and figure 21 present the distribution of the differences in gravity disturbances. Figure 20 is based on data of EGM96 subtracted from *reduced dynamic* data while figure 21 shows the difference, EGM96 subtracted from *kinematic* data.

The differences are plotted on the horizontal axis with unit mgal and the height of each bar indicates how often a certain difference occurs. The width of each bar equals 0.8, so that the centre bar, for example, counts the differences between ±0.4mgal.

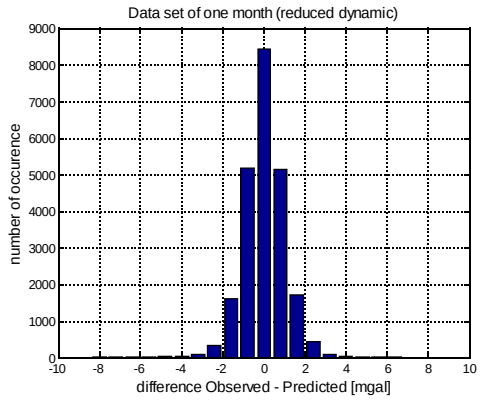

figure 20: distribution of gravity disturbances (reduced dynamic)

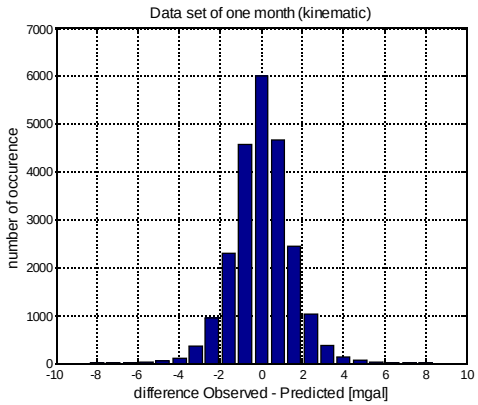

figure 21: distribution of gravity disturbances (kinematic)

The form of a normal distribution can immediately be seen in both figures although there is not an exact normal distribution which would be axis-symmetrical. However, the above distributions fulfill the requirements of the error estimation which interprets data as normal distributed.

The higher the magnitude of difference the lesser it occurs. This can be stated for both histograms (figure 20 and figure 21). On the other hand it can be distinguished that *reduced dynamic* data are more similar to EGM96 than *kinematic*. Approximately 8500 versus 6000 differences occur respectively in the centre interval.

It should be mentioned that similar distributions to figure 20 and figure 21 appear if the data are presented on a weekly scale instead of using data of the whole month. This strengthen the statement that the data can be interpreted as normal distributed.

The exact values of the gravity disturbances and their differences to EGM96 are described in mgal as mean, standard deviation, maximum and minimum values in table 16 and table 17. Those tables show a section of the GEOCOL output file where the last four digits have been eliminated (appendix C). The first table is derived from *reduced dynamic* calculations, the latter one from *kinematic* calculations.

table 16

COMPARISON OF PREDICTIONS AND OBSERVATIONS

DATA TYPE = 12

NUMBER: 23200

	OBSERVATIONS	PREDICTIONS	DIFFERENCE	
MEAN	-0.58	-0.59	0.01	0.3
ST.DEV.	14.05	14.02	1.01	0.0
MAX	37.41	36.28	6.68	0.3
MIN	-53.46	-52.24	-7.84	0.3

table 17

COMPARISON OF PREDICTIONS AND OBSERVATIONS

DATA TYPE = 12

NUMBER: 23200

	OBSERVATIONS	PREDICTIONS	DIFFERENCE	
MEAN	-0.56	-0.59	0.03	1.0
ST.DEV.	14.09	14.02	1.41	0.0
MAX	37.82	36.28	9.26	1.0
MIN	-53.00	-52.24	-8.22	1.0

DATA TYPE holds the code number 12 which states that gravity disturbances are presented. *NUMBER* declares the total number of observations. The last column contains the standard deviation of differences to EGM96 which was predefined by the user (compare section 4.3 and table 11 and table 12).

These standard deviations are lower than the standard deviations of *DIFFERENCEs* in column three although they should be almost identical. This aberration can be explained by the fact that the *DIFFERENCEs* are differences with respect to EGM96 to degree 24 while the last column are values derived from EGM96 to degree 360. The predefined standard deviations were however not altered during the processing of the program.

The differences in gravity disturbance compared to EGM96, as computed in GEOCOL, can be presented in a map of the earth. Figure 22 has been created

with GMT [Wessel and Smith 1998] (appendix A). The upper map shows how *reduced dynamic* gravity disturbances vary from the reference model while the lower map presents the same comparison with *kinematic* data.

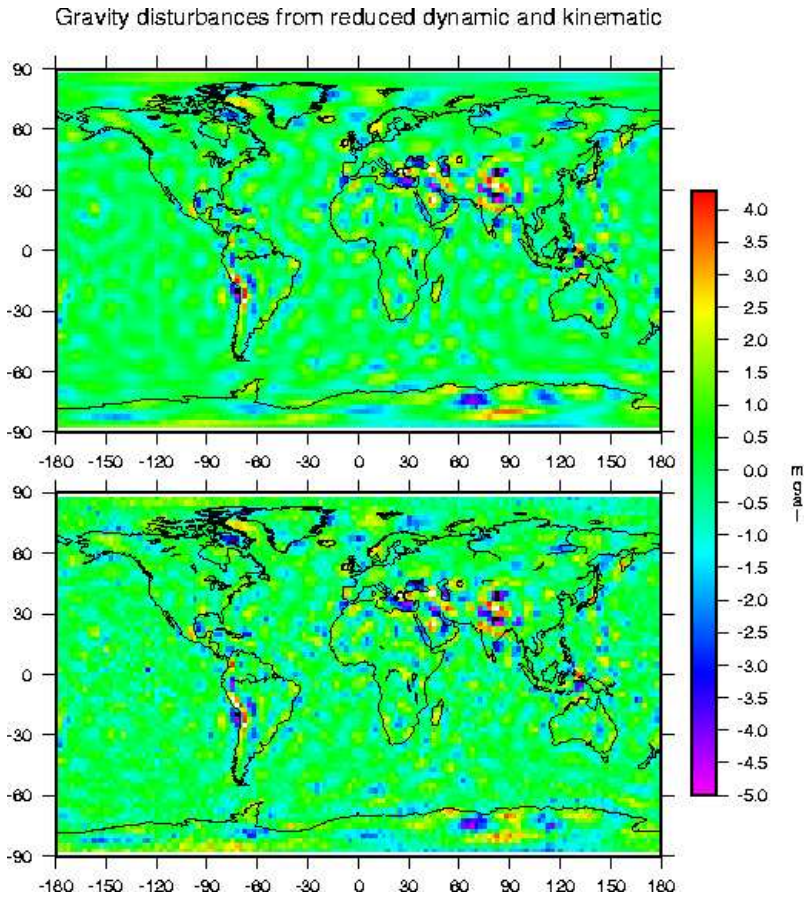

figure 22: gravity disturbances compared to EGM96

Most parts of the maps are green in colour which indicates that the differences lie in between -0.5mgal and 1.5mgal. The *kinematic* data show higher differences than the *reduced dynamic* data. As these differences do not create a specific pattern but are mostly equally spread they are assumed to be noise. Those observations ascertain the results from table 11 and table 12 in section 4.3.

Both maps of figure 22 have in common that certain areas, such as the Himalayas, Antarctica and the Andes show extreme differences (either around 4mgal or -5mgal). All these specific areas are difficult to access due to topographical reasons. Not many gravity measurements have therefore taken place in those areas. Since this lack of data is reflected in EGM96 it can be

assumed that gravity disturbances derived from CHAMP observations are more accurate than from the reference model in those places. Large differences appear as a consequence. Figure 22 encourages the idea that low orbiting satellites are generally able to provide information which would otherwise be very difficult to gain.

7.2 Spherical harmonic coefficients

Spherical harmonic coefficients are obtained by using collocation. An important question is now if these coefficients are consistent to the known. A consistency requires that the standard deviations of coefficient differences (CHAMP – EGM96) are smaller than the standard deviations of the coefficients of EGM96 themselves.

In order to judge the results of collocation, figure 23 represents data of the GEOCOL output file. The standard deviation is plotted on the vertical axis while the degree of coefficients is plotted on the horizontal axis. The standard deviations of coefficients are combined to one standard deviation per degree.

Following graphs are shown (figure 23):

- in red: standard deviations of coefficient differences (*reduced dynamic*-EGM96)
- in blue: standard deviations of coefficient differences (*kinematic*-EGM96)
- in green: standard deviations of coefficients from the energy conservation method
- in brown: standard deviations of coefficients of EGM96
- in cyan: standard deviation of estimated error of *reduced dynamic* coefficients
- in black: standard deviation of estimated error of *kinematic* coefficients

Up to degree 24, EGM96 has been removed from all data (compare section 5.3.2) therefore the standard deviation of EGM96 initially becomes zero and the standard deviations of the other data are very small for the first 24 degrees. It is obvious that only the residual standard deviations from degree one to 24 are calculated because only residual coefficients of those degrees are regarded.

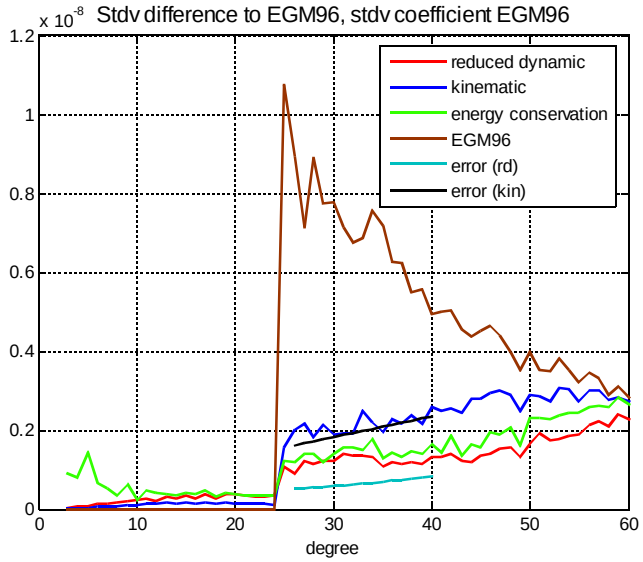

figure 23: comparison of gravity field models

At degree 25 the standard deviation of EGM96 (brown graph) shows its maximum. From that point on, the standard deviations of EGM96 coefficients decreases.

The opposite appears for the difference between EGM96 and CHAMP data (red and blue graph). The higher the degree the more oscillating errors can be observed in the coefficients derived from CHAMP data. As a consequence the standard deviation of differences to EGM96 increases towards higher degrees. However, this increase is slower than the decrease of the standard deviation of EGM96 coefficients (brown graph).

As long as the red and the blue graph are lower than the brown graph, a consistency in comparison to EGM96 is achieved. Calculations are carried out up to degree 60. At this degree, there is an intersection between the blue and brown graph which means that the kinematic data do not give information for a better resolution than 60 degree. The *reduced dynamic* differences, however, are always smaller than the *kinematic* and could as a consequence go a bit further than degree 60.

The results of the energy conservation method (green graph) refer to the *reduced dynamic* data set. Their standard deviations are similar to those derived from accelerations (red graph) but always a bit higher. The energy conservation method has also a noticeable problem with the low degree coefficients. The standard deviations of differences are high in the beginning bearing in mind that EGM96 is removed. This problem does not occur for the graphs based on accelerations (red and blue).

Error estimation

Figure 23 also shows the results of the error estimations in GEOCOL (equation 5.20). In both cases, *reduced dynamic* (cyan) and *kinematic* (black), the standard deviations of the errors are too optimistic in comparison to the evaluated standard deviations of the differences between EGM96 and CHAMP observations.

This can be partly explained by the fact that within the error estimation EGM96 is expected to have a standard deviation of zero while the calculated differences of standard deviations from EGM96 and CHAMP data are influenced by the real standard deviations of EGM96.

However, the main reason why the error estimation of the *reduced dynamic* data (cyan) is much too optimistic is that the user predefined noise of 0.3mgal (table 11) was too low.

Asides from these observations, the errors and standard deviations of differences are consistent.

If one takes a closer look at the error estimation of spherical harmonic coefficients that all belong to the same degree, the result will look like figure 24. It shows the errors of coefficients belonging to degree 35 and based on *reduced dynamic* observations. Coefficients of other degrees or based on *kinematic* data result in similar figures.

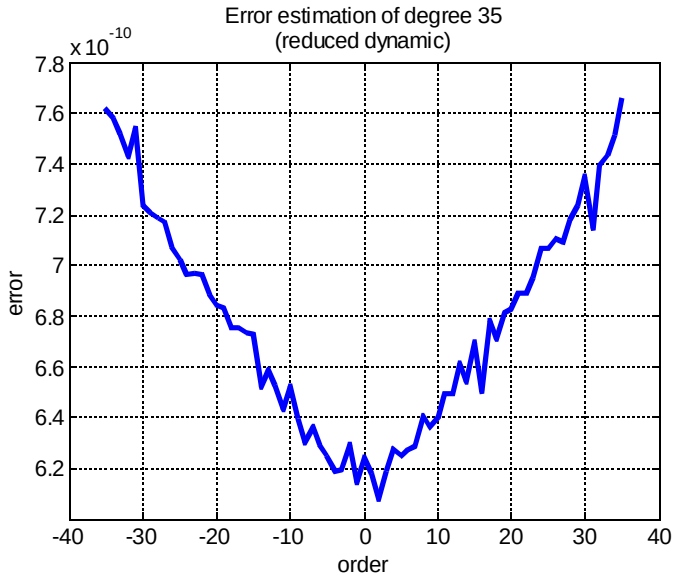

figure 24: error estimation of degree 35

Figure 24 shows that the minimal error occurs around order zero. The higher the magnitude of the order, the more the error increases. This kind of curvature is caused by the lack of satellite measurements in polar regions. Simulations exist which show that the errors of coefficients will present a horizontal line if they are derived from data which are fully distributed over the whole earth. Since CHAMP does not completely cover the poles, one must keep in mind that coefficients of higher orders have higher errors.

8 Conclusion

The main task to calculate a gravity field model using CHAMP data has successfully been carried out. The combination of Newton Interpolation and Least-Squares Collocation presents satisfying results. A reasonable gravity field model up to degree 60 has been created.

The conclusion can be drawn that the computation of spherical harmonic coefficients based on accelerations show an improvement of the gravity field model based on energy conservation.

One has also seen that the *reduced dynamic* data are less influenced by noise than the *kinematic* data if EGM96 is defined as a reference. It is therefore advisable to use the combination of *reduced dynamic* and *kinematic* data during the preprocessing step and then to carry on with only the filtered *reduced dynamic* data set.

However, the above conclusions are only derived from one-third of the observations of one month. More reliable conclusions can be drawn if more observed data are involved.

As the Least-Squares Collocation cannot handle much larger data sets, one possibility is to use Fast Spherical Collocation instead. This requires that the data are converted into gridded values of the same height.

Further investigations accounting for larger data sets should be done to see if similar results, to the one in this study, will be observed and more importantly, if a higher accuracy and resolution of the estimated gravity field model can be achieved.

References

[Austen and Reubelt 2000] Austen, G. and Reubelt, T.: Spatial gravity field analysis using semi-continuous ephemerides of low-orbiting GPS-tracked satellites of type CHAMP, GRACE and GOCE. Diploma Thesis, Institute of Geodesy, University of Stuttgart, http://www.uni-stuttgart.de/gi/education/diplomarbeiten/austen+reubelt.pdf, 2000.

[Blakely 1996] Blakely, R. J.: Potential Theory in Gravity & Magnetic Applications. Cambridge University Press, 1996.

[GFZ 2004] GeoForschungsZentrum Potsdam, http://www.gfz-potsdam.de/pb1/op/champ, 2004.

[Heiskanen and Moritz 1996] Heiskanen, W. A. and Moritz, H.: Physical Geodesy. Reprint, Institute of Physical Geodesy, Technical University of Graz, Austria, 1996.

[Howe et al. 2003] Howe, E., Stenseng, L. and Tscherning, C. C.: Analysis of one month of CHAMP state vector and accelerometer data for the recovery of the gravity potential. Advances in Geoscience, 1, 1-4, 2003.

[Jekeli 1999] Jekeli, C.: The determination of gravitational potential differences from satellite-to-satellite tracking. Celestial Mechanics and Dynamical Astronomy, 75, 85-101, 1999.

[Keller 2002] Keller, W.: Numerische Methoden für Geodäten. Lecture notes, Institute of Geodesy, University of Stuttgart, 22-24, 2002.

[Knudsen 1987] Knudsen, P.: Estimation and modelling of the local empirical covariance function using gravity and satellite altimeter data. Bulletin Géodésique, 61, 145-160, 1987.

[Lemoine et al. 1998] Lemoine, F., Kenyon, S., Factor, J., Trimmer, R., Pavlis, N., Chinn, D., Cox, C., Klosko, S., Luthcke, S., Torrence, M., Wang, Y., Williamson, R., Pavlis, E., Rapp, R., and Olson, T.: The development of the joint NASA GSFC and the national imagery and mapping agency (NIMA) geopotential model EGM96. Tech. Rep. NASA/TP-1998-206861, NASA Goddard Space Flight Center, 1998.

[Longman 1959] Longman, I.: Formulas for computing the tidal accelerations due to the moon and the sun. Journal of Geophysical Research, 64, 2351-2355, 1959.

[Montenbruck and Gill 2001] Montenbruck, O. and Gill, E.: Satellite Orbits: Models, Methods, and Applications. Springer, 2001.

[Moritz 1980] Advanced physical geodesy. Karlsruhe: Wichmann, 1980.

[Sansó and Tscherning 2003] Sansó, F. and Tscherning, C. C.: Fast Spherical Collocation - Theory and Examples. Journal of Geodesy, 77, 101-112, DOI 10.1007/s00190-002-0310-5, 2003.

[Seeber 1993] Seeber, G.: Satellite Geodesy: foundations, methods and applications. de Gruyter, 1993.

[Tscherning 1974] Tscherning, C. C.: A FORTRAN IV Program for the Determination of the Anomalous Potential Using Stepwise Least Squares Collocation. Reports of the Department of Geodetic Science No. 212, The Ohio State, University, Columbus, Ohio, 1974.

[Tscherning et al. 1994] Tscherning, C. C., Knudsen, P. and Forsberg, R.: Description of the GRAVSOFT package. Geophysical Institute, University of Copenhagen, Technical Report, http://cct.gfy.ku.dk ,1991, 2. Ed. 1992, 3. Ed. 1993, 4. Ed, 1994.

[Tscherning 2001] Tscherning, C. C.: Computation of spherical harmonic coefficients and their error estimates using Least-Squares Collocation. Journal of Geodesy, 75, 12-18, 2001.

[Wessel and Smith 1998] Wessel, P. and Smith, WHF.: New improved version of Generic Mapping Tools released. EOS Trans. American Geophysical Union, 79 (47), 579, 1998.

Appendix A

GMT source files

```
# source file of figure 19
#!/bin/csh -f

gmtset ANOT_FONT Times-Bold ANOT_FONT_SIZE 10
gmtset LABEL_FONT Times-Bold LABEL_FONT_SIZE 6
gmtset DEGREE_FORMAT 3

set region = -180/180/-90/90   # define the considered area
set output = tracks.ps         # name the output file

# Make a file withthe tracks to plot
     awk  '{print  $3,$2}'  /disk1/tin/GMT_track/GMT_input_mod2_rd.txt  >!
track

#  Initiate the plot with lat/lon limits and add coast lines:
           pscoast  -R$region -JX20c/10c  -B30WenS  -A0.25  -G230/250/220  -K
>! $output

# add some text to the figure
pstext  -R  -JX -N -O -K -G0/150/0 << END >> $output
0 100 12 0 0 CT CHAMP GROUND TRACK, 1 Month.
END

# add the tracks to the figure
psxy  track  -R  -JX -O  -Sc0.05 -G0/0/250  >> $output

#ps2epsi $output

     \rm .gmtcommands track
```

```
# source file of figure 22
#!/bin/csh

gmtset ANOT_FONT Helvetica ANOT_FONT_SIZE 8p
gmtset LABEL_FONT Helvetica LABEL_FONT_SIZE 8p
gmtset PAPER_MEDIA A4

set region = -180/180/-90/90
set output = "anomalies_rd_k.ps"

awk '{print $3,$2,$6}' /disk1/tin/GMT_grav/anomalies_total_k.dat | \
 xyz2grd -Gucph-egm96.grd -R-180/180/-87.5/87.5 -I2.5

awk '{print $3,$2,$6}'  /disk1/tin/GMT_grav/anomalies_total_rd.dat| \
 xyz2grd -Gucph-eigen2.grd -R-180/180/-87.5/87.5 -I2.5

makecpt -Crainbow -T-5.0/4.3/0.1 -Z >! champ.cpt

grdimage ucph-egm96.grd -JX10c/6c -R$region -B30WenS -Cchamp.cpt \
 -K -P >! $output

psscale -Cchamp.cpt  -D10.5/6/10c/0.4c -B1 -B0.5:"mgal": -O -K >> $output

pscoast -JX -R -Dc -O -W3 -B30WenS -A10000 -K >> $output

grdimage ucph-eigen2.grd -JX10c/6c -R$region -B30WenS -Cchamp.cpt \
 -K -O -Y7c >> $output

pscoast -JX -R -Dc -O -W3 -B30WenS -A10000 -K >> $output

echo "0 90 11 0 0 CT Gravity disturbances from reduced dynamic and
kinematic" | \pstext -JX -R -O -Y1c >> $output

gv anomalies_rd_k.ps

ps2epsi $output

#/rm ucph-egm96.grd ucph-eigen2.grd champ.cpt
```

Appendix B

GEOCOL job-files

```
/cct/dgravsoft/geocol16<<!
t
t f t t f f f f
4
/scratch/tin/neq1
40 300
/scratch/tin/neq2
41 300
/scratch/tin/neq3
42 300
/scratch/tin/neq4
43 300
f t f f f f f f
t
5
EGM96 TO DEGREE 24
3.986004415E+14  6378136.3 0.0 24 f f t f f
(2i4,2d20.12)
/cct/cctf/EGM96
2
4
-1.561  540.9  24 f F t F
-1 2 1.03
/cct/dgravsoft/egm96.edg
t
 -1 2 3 5 4  5 0  12 -1 413000.0 f f F T f t t f f t
/disk1/tin/geocol_input3.txt
29
2.5
1.0E5 0.0 t
0.3
t
t f
f f
t f t t
3 0
60 60
/disk1/tin/EGM96_25
(2i4,2d20.12)
t
t
```

```
/cct/dgravsoft/geocol16<<!
t
t f t t f f f f
4
/scratch/tin/neq1
40 300
/scratch/tin/neq2
41 300
/scratch/tin/neq3
42 300
/scratch/tin/neq4
43 300
f t f f f f f f
t
5
EGM96 TO DEGREE 24
3.986004415E+14  6378136.3 0.0 24 f f t f f
(2i4,2d20.12)
/cct/cctf/EGM96
2
4
-1.561  540.9  24 f F t F
-1 2 1.03
/cct/dgravsoft/egm96.edg
t
 -1 2 3 5 4  5 0  12 -1 413000.0 f f F T f t t f f t
/disk1/tin/geocol_input3.txt
29
2.5
1.0E5 0.0 t
0.3
t
t t
t 23200
f f
t t t t
33 -33
40 40
/disk1/tin/EGM96_25
(2i4,2d20.12)
t
t
```

Appendix C

GEOCOL output file

```
 GEODETIC COLLOCATION, VERSION 2003-03-11 RELEASE 16 REV. 11 exp (LINUX)
 Thu Dec  2 10:10:31 2004

 NOTE THAT IF SPHERICAL APPROXIMATION IS USED
 MEAN RADIUS = RE = 6371 KM AND MEAN GRAVITY 981 KGAL USED.


 MAX NUMBER OF OBS PER RECORD = 5600, MAX NUMBER OF PARAMETERS= 2500
 MAX NUMBER OF DATA DEPENDING ON TILT-PARAMETER  100002
 SIZE OF NORMAL EQ. BLOCKS= 399120, SIZE OF POT.COFF. BLOCK= 3243602
  INTERACTIVE INPUT (T/F)
  BUFFER SIZE MAXO9 =       403200
 INPUT: LSPHER, TRUE IF SPHERICAL APPROXIMATION IS USED.
        LTRAN, TRUE IF NON-STANDARD REF. SYSTEM IS USED
        LPOT,  TRUE IF SPHERICAL HARMONIC EXPANSION IS USED
        LTEST, TRUE IF TEST-OUTPUT IS NEEDED
        LLEG,  TRUE IF LEGEND IS TO BE OUTPUT
        LPARAM,TRUE IF PARAMETERS ARE TO BE DETERMINED
        LNCOL, TRUE IF COLLOCATION IS NOT USED
        LIOSOL,TRUE IF SOLUTION IS STORED OR RECOVERED
  SPHERICAL APPROXIMATION IN USE.
           21 BLOCKS IN EACH FILE NEEDED
  INPUT NUMBER OF FILES TO HOLD NEQ
  INPUT NAME OF FILE WITH NORMAL EQ.
 NAME OF FILE HOLDING NORMAL EQUATIONS=/scratch/tin/neq1
  INPUT FORTRAN UNIT NO (> 20) AND SIZE IN  BLOCKS
           40         300
  INPUT NAME OF FILE WITH NORMAL EQ.
 NAME OF FILE HOLDING NORMAL EQUATIONS=/scratch/tin/neq2
  INPUT FORTRAN UNIT NO (> 20) AND SIZE IN  BLOCKS
           41         300
  INPUT NAME OF FILE WITH NORMAL EQ.
 NAME OF FILE HOLDING NORMAL EQUATIONS=/scratch/tin/neq3
  INPUT FORTRAN UNIT NO (> 20) AND SIZE IN  BLOCKS
           42         300
  INPUT NAME OF FILE WITH NORMAL EQ.
 NAME OF FILE HOLDING NORMAL EQUATIONS=/scratch/tin/neq4
  INPUT FORTRAN UNIT NO (> 20) AND SIZE IN  BLOCKS
           43         300
 INPUT: LONEQ, TRUE IF COEFFICIENTS ARE OUTPUT,
        LTIME: TRUE, IF TIMING IS MADE (ONLY UNIX)
        LTCOV: TRUE, IF OUTPUT FROM COV. CALCULATION
        LCZERO: TRUE, IF  FINITE COVARIANCES ARE USED
                IN NORMAL EQUATIONS.
        LCOERR: TRUE, IF DATA ERRORS ARE CORRELATED.
        LFULLO: TRUE, IF V, ALL COM. OF DG OR DDG ARE OUTPUT
  ARE ALL PARAMETERS OK ?
 INPUT CODE FOR BASIC REFERENCE SYSTEM:
 0: USER DEFINED, 1: ED50 NORTH SEA, 2: ED50/EDOC,
 3: NAD1927 /NEW MEXICO, 4: GRS67, 5:  GRS80, 6: NWL9D,
 7: BEST CURRENT, 8: BEST CUR. FAROE ISL, 9: ED50 FOR SF,
 10: IAG-75, 11: KRASSOWSKY, DDR, 12: GERMAN DHDN, BESS.

  REFERENCE SYSTEM:
 +                  GRS1980.

  A   = 6378137.00 M
  1/F = 298.2572204
  GM= 0.3986005000E+15
  REF.GRAVITY AT EQUATOR =   978032.6772 MGAL
  POTENTIAL AT REF.ELL.  = 62636860.8504 M**2/SEC**2

   INPUT NAME OF POT.COEFF. SET
```

```
 SOURCE OF THE POTENTIAL COEFFICIENTS USED:
 EGM96 TO DEGREE 24
 INPUT: GM, SEMI-MAJOR AXIS (M), C(2,0), MAX. DEGREE
  LFM, TRUE IF COEFF. IN INPUT STREEM AND *1.0D6
  LBIN, TRUE IF ON BINARY FORM
  LFORM, TRUE IF FORMAT IS INPUT
  LINT, TRUE IF STORED AS INTEGERS
  LSKIPL, TRUE IF DUMMY LINES IN FRONT OF FILE


     GM             A       COFF(5)  MAX.DEGREE
 0.39860044E+15  6378136.3    0.0000   24
  INPUT FORMAT (2I4,2D18.0) F.EX.
  INPUT NAME OF FILE HOLDING COEFF.
 NAME OF FILE HOLDING COEFFICIENTS: /cct/cctf/EGM96
  COEFFICIENTS UP TO N=5
    2   0 -0.484165360E-03  0.000000000E+00
    2   1 -0.186987630E-09  0.119528010E-08
    2   2  0.243914360E-05 -0.140016690E-05
    3   0  0.957254200E-06  0.000000000E+00
    3   1  0.202998880E-05  0.248513150E-06
    3   2  0.904627770E-06 -0.619025970E-06
    3   3  0.721072640E-06  0.141435620E-05
    4   0  0.539873840E-06  0.000000000E+00
    4   1 -0.536321640E-06 -0.473440250E-06
    4   2  0.350694110E-06  0.662671600E-06
    4   3  0.990771810E-06 -0.200928370E-06
    4   4 -0.188560800E-06  0.308853170E-06

 START OF COLLOCATION I:
  INPUT DEGREE-VARIANCE MODEL NO. (1,2,3)
  INPUT DENOMINATOR(S) IN MODEL

 THE MODEL ANOMALY DEGREE-VARIANCES ARE EQUAL TO
 A*(I-1)
+        /((I-2)*(I+   4)).
 INPUT PARAMETERS DESCRIBING COV. FCT.
 R - NEG. DEPTH TO BJ.SPHERE IN KM OR RATIO RB/RE
 GRAVITY ANOMALY VARIANCE IN MGAL**2
 MAX. DEGREE OF LEGENDRE FCT. EXPANSION (E.G. 180, 360)
 LZERO - TRUE IF FIRST COEFF. ALL ARE ZERO
 LTABLE - TRUE IF COV.FCT. IS TABULATED IN 2D
 LMODEL - TRUE IF DEGREE-VAR. FROM PREDEFINED MODEL
 LTABH - TRUE IF 1D TABULATION
 HCMAX =  1000000.0 M.
  INPUT MODEL NO., START DEGR. & SCALE FACT.
 MODEL  -1 USED FROM DEGREE   2 TO  24 WITH SCALE FACTOR=  1.030000
  INPUT NAME OF FILE WITH DEGR.VAR.
  DEGREE-VARIANCES INPUT FROM FILE
 /cct/dgravsoft/egm96.edg
  MULTIPLICATIVE FACTOR USED

 RATIO R/RE                              =       0.999755
 DEPTH TO BJERHAMMAR SPHERE (R-RE)       =   -1561.00 M
 VARIANCE OF POINT GRAVITY ANOMALIES     =     540.90 MGAL**2
 THE FACTOR A, DIVEDED BY RE**2 IS       =     144.23 MGAL**2
  ARE ALL PARAMETERS OK ?

 TIME USED=    0.000 SEC, ELAPSED TIME =     0.000 SEC

  OBSERVATIONS:
```

```
 INPUT DATA LINE AND OUTPUT SPECIFICATIONS
 POSITION OF STATION NUMBER (0: NO NUMBER, -1: NO OUTPUT U6)
 POSITION OF LATITUDE AND LONGITUDE (E.G. 2 , 3)
 TYPE OF ANGULAR UNITS USED (1: DD MM SS.S, 2: DD MM.M 3: DD.D)
 4: GRADES, 5: X,Y,Z (CTRS)
 POSITION OF HEIGHT (0: NO HEIGHT)
 POSITION OF OBSERVATION 1 AND 2 (0 IF NO OBS. 1 OR 2)
 DATA OR COMPUTATION QUANTITY TYPE CODE (11: GEOID,
   13: GRAVITY, 15: TZZ, 26: (KSI,ETA), NEGATIVE: REF.SUBTR.)
 COORD.SYST. CODE, -1 INDICATE GLOBAL SYSTEM, +100 REVERSE TR.
 HEIGHT (IN M OR KM), ONLY USED IF NO INPUT HEIGHT
 (USED AS HEIGHT ABOVE MEAN EARTH SPHERE IF LSPHER IS TRUE !)
 LPUNCH - TRUE IF OUTPUT OF RESULT TO FILE
 LWLONG - TRUE IF LONGITUDE POSITIVE EAST
 LMEAN  - OBS. OR COMPUTED QUANTITY IS A MEAN VALUE
 LSA    - TRUE IF ALL ERROR ESTIMATES ARE IDENTICAL
 LKM    - TRUE IF HEIGHT IN KM
 LADMU  - TRUE IF UNREDUCED OR CONSTANTS * OR +
 STAT   - TRUE IF STATISTICS OF RESULT WANTED
 LAREA  - TRUE IF DATA ONLY INSIDE SPECIFIC AREA ARE USED
 LFORM  - TRUE IF FORMAT OF DATA IS INPUT
 LIN4   - TRUE IF DATA NOT IN INPUT STREAM (FROM FILE)
  INPUT NAME OF FILE HOLDING DATA
  INPUT FORTRAN UNIT NUMBER

 DATA INPUT FROM UNIT 29, FILE=/disk1/tin/geocol_input3.txt
  INPUT SAMPLING INTERVAL SIZE
 INPUT MULTIPLICATIVE AND ADDITIVE CONSTANT AND
 LMEGR, TRUE IF VALUE INPUT OR COMPUTED IS UNREDUCED
 DM=      0.10000D+06, DA=      0.00000D+00, LMEGR=  T
  INPUT COMMON STANDARD DEVIATION OF OBSERVATIONS
 COMMON ST.DEV. OF OBS =   0.3000
  ALL SPECIFICATIONS OK ?


 SELECTED GEOCENTRIC SYSTEM USED.


    NO      LATITUDE     LONGITUDE     H    GRA.DIST. MGAL
             DEGREES       DEGREES      M
+                                              ST.DEV.=    1.168280
                                                                  POT
+                                              OBS    DIF    ERR
 ONLY STATION NUMBERS OUTPUT:
      118877     118967     119057     119147     119237     119327
      119417     119507     119597     119687     119777     119867
      119957     120047     120137     120227     120317     120407

                                    [...]

      654287     654377     654467     654557     654647     654737
      655187     655277     655367     655457     655547     655637
      655727     655817     655907     655997     656087     656177
 NUMBER OF OBSERVATIONS REQUIRE STORAGE ON UNIT 14 AND 16
  ROTSATX   0.0000000000000000E+000  0.0000000000000000E+000
  3 BLOCK            1 WRITTEN, LSATAC=  F
      656267     656357     656447     656537     656627     656717
      656807     656897     656987     657077     657167     657257
      657347     657437     657527     657617     657707     657797

                                    [...]

     2591027    2591117    2591207    2591297    2591387    2591477
```

```
     2591567    2591657    2591747    2591837
  INPUT LSTOP, LRESOL _ READ SOLUTION
0COMPARISON OF PREDICTIONS AND OBSERVATIONS
0DATA TYPE = 12
 NUMBER: 23200
0         OBSERVATIONS     PREDICTIONS     DIFFERENCE
 MEAN        -0.579111       -0.591064        0.011953        0.300000
 ST.DEV.     14.049431       14.015602        1.010206        0.000000
 MAX         37.414601       36.276459        6.680018        0.300000
 MIN        -53.460592      -52.239471       -7.840071        0.300000
0DISTRIBUTION OF DIFFERENCES, UNITS:  2.500000
   0  0  0  0  0  0  0  9 69********* 62  3  0  0  0  0  0  0  0       0
 -10 -9 -8 -7 -6 -5 -4 -3 -2 -1  0  1  2  3  4  5  6  7  8  9 10 OUTSIDE


 NUMBER OF DIFF. REPEATED
     0     0     0     0     0     0     0     9    69  1871 19100  2086
62     3     0     0     0     0     0     0     0     0
           5 BLOCKS STORED

 TIME USED=    1.170 SEC, ELAPSED TIME =     1.220 SEC
  FILE           40 OPENED FOR NEQ
  FILE           41 OPENED FOR NEQ
  FILE           42 OPENED FOR NEQ
  FILE           43 OPENED FOR NEQ
           4 FILE(S) OPENED FOR NEQ

    688 RECORDS USED FOR NORMAL EQUATIONS.

          100 BLOCKS WRITTEN
          200 BLOCKS WRITTEN
          300 BLOCKS WRITTEN
          400 BLOCKS WRITTEN
          500 BLOCKS WRITTEN
          600 BLOCKS WRITTEN
 TIME USED= 849.680 SEC, ELAPSED TIME= 947.510 SEC
  REDUCED BLOCK            1 WRITTEN, LAST CO.          878
  REDUCED BLOCK            2 WRITTEN, LAST CO.         1252
  REDUCED BLOCK            3 WRITTEN, LAST CO.         1538

                                  [...]

  REDUCED BLOCK          687 WRITTEN, LAST CO.        23187
  REDUCED BLOCK          688 WRITTEN, LAST CO.        23201
  1 BLOCK            1 WRITTEN
  1 BLOCK            2 WRITTEN
  1 BLOCK            3 WRITTEN
  1 BLOCK            4 WRITTEN
  1 BLOCK            5 WRITTEN

 SOLUTIONS TO NORMAL EQUATIONS:

 BLK            1 10 READ FOR TRANSFER B TO C.
 BLK            1 11 READ FOR TRANSFER B TO C.
 ONLY FIRST   20 SOLUTIONS OUTPUT.
  0.473534491E+01 0.283777113E+01 0.528241753E+01 0.460102119E+01
  0.184944313E+01 0.351367335E+01 0.251701313E+01 0.223070890E+01
  0.286572101E+01 0.275005284E+01 0.229883985E+01 0.261306913E+01
  0.251107169E+01 0.282136379E+01 0.289944247E+01 0.262643399E+01
  0.387554148E+01 0.464294867E+01 0.308888872E+01 0.371346221E+01

 NUMBER OF EQUATIONS =  23200
 NORMALIZED SQUARE-SUM OF OBSERVATIONS        = 0.173482E+05
```

```
 NORMALIZED DIFFERENCE BETWEEN SQUARE-SUM OF
 OBSERVATIONS AND NORM OF APPROXIMATION       = 0.485372E+04

 TIME USED=******** SEC, ELAPSED TIME=******** SEC
  NUMBER OF BLOCKS USED =          688
 INPUT LCREF, TRUE IF ANOTHER COLLOCATION SOLUTION IS NEEDED
       LNEWDA, TRUE IF PARAMETERS ARE TO BE DETERMINED
  LTEST  T
  PREDICTIONS: <

 INPUT: LGRID - TRUE IF COMPUTATIONS IN A GRID
  OR WHEN LSPHAR IS TRUE ALL COEFF. LE THE DEGREE
  LERR - TRUE IF ERROR ESTIMATES ARE TO BE COMPUTED
            OR REPRODUCED IN OUTPUT
  LCOMP- TRUE IF COMPUTED VALUES ARE SUBTRACTED FROM OBSERVED
  LSPHAR - TRUE IF COEFFICIENTS OF SPHERICAL HARMONICS ARE
            TO BE PREDICTED
  INPUT INITIAL DEGREE AND ORDER
  INITIAL DEGREE AND ORDER            3           0
  INPUT DEGREE & ORDER OF COEFF. TO BE PREDICTED
  LCOMP - OBS-PRED CALCULATED  T
  INPUT NAME OF COEFF. FILE FOR COMPARISON
  INPUT DATA FORMAT
(2i4,2d20.12)
  GRAVITY ANOMALY AND POTENTIAL DEG.VAR. DEG 3-200
   0.0000   0.0000   0.0000   0.0000   0.0000   0.0000   0.0001   0.0001
   0.0002   0.0004   0.0004   0.0006   0.0007   0.0010   0.0011   0.0015
   0.0017   0.0020   0.0023   0.0025   0.0029   0.0034   0.0041   5.1239
   4.9421   4.7727   4.6144   4.4663   4.3272   4.1966   4.0734   3.9573

                                    [...]

   0.0003   0.0003   0.0003   0.0002   0.0002   0.0002   0.0002   0.0002
   0.0002   0.0002   0.0002   0.0002   0.0002   0.0002   0.0002   0.0002
   0.0002   0.0002   0.0002   0.0002   0.0002   0.0002
   3   0    0.20265D-11    0.00000D+00    0.20265D-11
   3   1   -0.30350D-10    0.00000D+00   -0.30350D-10
   3   2   -0.71487D-11    0.00000D+00   -0.71487D-11
   3   3    0.31209D-10    0.00000D+00    0.31209D-10
 MEAN, STDV, VARI=     -0.60905D-12     0.18017D-10     0.16692D-10
 MEAN COLL ERR=      0.00000D+00 COEFF. STDV.      0.00000D+00

   4  -4    0.50792D-11    0.00000D+00    0.50792D-11
   4  -3   -0.12031D-10    0.00000D+00   -0.12031D-10
   4  -2   -0.20574D-10    0.00000D+00   -0.20574D-10
   4  -1   -0.93529D-10    0.00000D+00   -0.93529D-10
   4   0    0.13577D-09    0.00000D+00    0.13577D-09
   4   1    0.37368D-10    0.00000D+00    0.37368D-10
   4   2    0.14226D-10    0.00000D+00    0.14226D-10
   4   3    0.29587D-11    0.00000D+00    0.29587D-11
   4   4   -0.21308D-11    0.00000D+00   -0.21308D-11
 MEAN, STDV, VARI=      0.74599D-11     0.60090D-10     0.57143D-10
 MEAN COLL ERR=      0.00000D+00 COEFF. STDV.      0.00000D+00

   5  -5    0.30012D-10    0.00000D+00    0.30012D-10
   5  -4   -0.17304D-10    0.00000D+00   -0.17304D-10
   5  -3    0.20753D-10    0.00000D+00    0.20753D-10
   5  -2   -0.10262D-10    0.00000D+00   -0.10262D-10
   5  -1   -0.80934D-10    0.00000D+00   -0.80934D-10
   5   0   -0.63810D-10    0.00000D+00   -0.63810D-10
   5   1   -0.56693D-10    0.00000D+00   -0.56693D-10
   5   2   -0.35792D-10    0.00000D+00   -0.35792D-10
   5   3   -0.88163D-11    0.00000D+00   -0.88163D-11
```

```
  5   4    0.68400D-10    0.00000D+00    0.68400D-10
  5   5   -0.44764D-10    0.00000D+00   -0.44764D-10
MEAN, STDV, VARI=     -0.18110D-10     0.44728D-10     0.46332D-10
MEAN COLL ERR=      0.00000D+00 COEFF. STDV.      0.00000D+00

  6  -6    0.18608D-10    0.00000D+00    0.18608D-10
  6  -5   -0.16632D-11    0.00000D+00   -0.16632D-11
  6  -4    0.22768D-10    0.00000D+00    0.22768D-10
  6  -3    0.16972D-10    0.00000D+00    0.16972D-10
  6  -2    0.34813D-10    0.00000D+00    0.34813D-10
  6  -1   -0.27102D-09    0.00000D+00   -0.27102D-09
  6   0    0.24761D-09    0.00000D+00    0.24761D-09
  6   1    0.16890D-09    0.00000D+00    0.16890D-09
  6   2    0.54584D-10    0.00000D+00    0.54584D-10
  6   3   -0.95426D-11    0.00000D+00   -0.95426D-11
  6   4    0.52054D-10    0.00000D+00    0.52054D-10
  6   5    0.37226D-11    0.00000D+00    0.37226D-11
  6   6   -0.23482D-10    0.00000D+00   -0.23482D-10
MEAN, STDV, VARI=      0.24178D-10     0.11705D-09     0.11503D-09
MEAN COLL ERR=      0.00000D+00 COEFF. STDV.      0.00000D+00

                                [...]

 35 -35   -0.55418D-08   -0.50123D-08   -0.52951D-09
 35 -34    0.31985D-08    0.26672D-08    0.53132D-09
 35 -33   -0.26688D-08   -0.30774D-08    0.40861D-09
 35 -32   -0.84140D-08   -0.74186D-08   -0.99543D-09
 35 -31    0.35824D-08    0.40412D-08   -0.45883D-09
 35 -30    0.24453D-08    0.28737D-08   -0.42843D-09
 35 -29    0.29271D-08    0.34014D-08   -0.47432D-09
 35 -28   -0.15440D-07   -0.15367D-07   -0.72237D-10
 35 -27   -0.13867D-07   -0.13381D-07   -0.48565D-09
 35 -26    0.50943D-08    0.46149D-08    0.47943D-09
 35 -25    0.10583D-08    0.19978D-08   -0.93955D-09
 35 -24    0.50576D-08    0.63850D-08   -0.13274D-08
 35 -23   -0.29348D-08   -0.22244D-08   -0.71042D-09
 35 -22    0.55059D-08    0.57230D-08   -0.21708D-09
 35 -21    0.84565D-10   -0.81766D-09    0.90222D-09
 35 -20   -0.18090D-08   -0.11357D-09   -0.16954D-08
 35 -19   -0.35684D-08   -0.34185D-08   -0.14984D-09
 35 -18   -0.11776D-07   -0.11471D-07   -0.30523D-09
 35 -17   -0.89931D-08   -0.88292D-08   -0.16394D-09
 35 -16   -0.69204D-08   -0.73683D-08    0.44791D-09
 35 -15    0.81308D-08    0.87598D-08   -0.62910D-09
 35 -14   -0.59856D-08   -0.70274D-08    0.10417D-08
 35 -13    0.61267D-08    0.30285D-08    0.30982D-08
 35 -12   -0.64008D-08   -0.64323D-08    0.31544D-10
 35 -11   -0.36229D-08   -0.31151D-08   -0.50785D-09
 35 -10    0.11396D-07    0.11444D-07   -0.48085D-10
 35  -9    0.42055D-09   -0.10878D-08    0.15084D-08
 35  -8    0.11848D-07    0.92149D-08    0.26330D-08
 35  -7    0.26861D-08    0.47139D-08   -0.20278D-08
 35  -6    0.83781D-08    0.79014D-08    0.47672D-09
 35  -5   -0.11023D-07   -0.11548D-07    0.52463D-09
 35  -4    0.10233D-07    0.92067D-08    0.10261D-08
 35  -3    0.24147D-08    0.34997D-08   -0.10850D-08
 35  -2    0.86051D-08    0.74732D-08    0.11320D-08
 35  -1   -0.10129D-07   -0.10358D-07    0.22825D-09
 35   0    0.76096D-08    0.86044D-08   -0.99485D-09
 35   1   -0.12109D-07   -0.10763D-07   -0.13463D-08
 35   2   -0.17858D-07   -0.14817D-07   -0.30410D-08
 35   3    0.25217D-08    0.18862D-08    0.63549D-09
 35   4   -0.32450D-08   -0.28234D-08   -0.42162D-09
```

```
 35   5   -0.88534D-08   -0.72369D-08   -0.16165D-08
 35   6    0.57152D-08    0.32871D-08    0.24281D-08
 35   7   -0.48857D-08   -0.34583D-08   -0.14274D-08
 35   8    0.18907D-08    0.41591D-08   -0.22684D-08
 35   9   -0.51098D-09   -0.78358D-09    0.27260D-09
 35  10   -0.23260D-08   -0.26308D-08    0.30480D-09
 35  11    0.29442D-08    0.31135D-08   -0.16929D-09
 35  12    0.96077D-08    0.81043D-08    0.15033D-08
 35  13   -0.10396D-08   -0.16087D-08    0.56911D-09
 35  14   -0.62146D-08   -0.71651D-08    0.95050D-09
 35  15   -0.14536D-07   -0.15369D-07    0.83347D-09
 35  16   -0.55850D-08   -0.68977D-08    0.13128D-08
 35  17    0.45733D-09    0.70376D-09   -0.24643D-09
 35  18   -0.61512D-08   -0.55525D-08   -0.59869D-09
 35  19   -0.44360D-09   -0.10711D-08    0.62753D-09
 35  20    0.49227D-09    0.99270D-09   -0.50043D-09
 35  21    0.12630D-07    0.12933D-07   -0.30307D-09
 35  22    0.65168D-08    0.75148D-08   -0.99801D-09
 35  23   -0.82173D-08   -0.81639D-08   -0.53340D-10
 35  24    0.37631D-08    0.27844D-08    0.97874D-09
 35  25    0.73267D-08    0.71686D-08    0.15815D-09
 35  26   -0.41013D-08   -0.47030D-08    0.60166D-09
 35  27    0.11478D-07    0.10960D-07    0.51773D-09
 35  28    0.73666D-08    0.78816D-08   -0.51504D-09
 35  29    0.74887D-08    0.77079D-08   -0.21915D-09
 35  30   -0.46773D-08   -0.40519D-08   -0.62542D-09
 35  31    0.82893D-08    0.78414D-08    0.44793D-09
 35  32   -0.35209D-08   -0.31627D-08   -0.35826D-09
 35  33    0.54855D-08    0.58610D-08   -0.37547D-09
 35  34   -0.86193D-09   -0.12163D-08    0.35440D-09
 35  35   -0.57840D-08   -0.58787D-08    0.94705D-10
MEAN, STDV, VARI=     -0.31954D-10     0.10569D-08     0.10499D-08
MEAN COLL ERR=      0.00000D+00 COEFF. STDV.      0.71715D-08

                                  [...]

 60 -60    0.19067D-08    0.39298D-09    0.15137D-08
 60 -59   -0.36884D-09    0.12059D-08   -0.15747D-08
 60 -58    0.14457D-08    0.23163D-08   -0.87060D-09
 60 -57    0.24104D-09   -0.32249D-09    0.56353D-09
 60 -56   -0.14207D-08   -0.35420D-08    0.21213D-08
 60 -55    0.15836D-08    0.28937D-08   -0.13102D-08
 60 -54   -0.11497D-08   -0.27101D-08    0.15604D-08
 60 -53    0.24584D-08    0.56805D-08   -0.32220D-08
 60 -52    0.32412D-08    0.53687D-08   -0.21275D-08
 60 -51   -0.24093D-08   -0.58027D-09   -0.18290D-08
 60 -50    0.26119D-08    0.38470D-08   -0.12351D-08
 60 -49   -0.16094D-08   -0.44639D-08    0.28545D-08
 60 -48   -0.15742D-08   -0.37264D-08    0.21523D-08
 60 -47    0.17281D-08    0.19792D-08   -0.25113D-09
 60 -46    0.19289D-09    0.34886D-09   -0.15597D-09
 60 -45   -0.27428D-08   -0.39178D-08    0.11749D-08
 60 -44   -0.16353D-09   -0.80850D-09    0.64497D-09
 60 -43   -0.40075D-11    0.79634D-09   -0.80035D-09
 60 -42    0.20289D-08    0.31044D-08   -0.10755D-08
 60 -41    0.10303D-08   -0.10469D-08    0.20771D-08
 60 -40   -0.23847D-09    0.95447D-09   -0.11929D-08
 60 -39   -0.21413D-08   -0.53656D-08    0.32243D-08
 60 -38   -0.10706D-08   -0.13266D-10   -0.10573D-08
 60 -37    0.17903D-08    0.71265D-09    0.10777D-08
 60 -36   -0.35641D-09   -0.49168D-10   -0.30724D-09
 60 -35    0.18009D-09    0.56185D-09   -0.38177D-09
 60 -34   -0.76969D-09   -0.23693D-08    0.15996D-08
```

60	-33	0.16908D-08	0.40229D-08	-0.23320D-08
60	-32	-0.46162D-09	-0.31556D-09	-0.14605D-09
60	-31	0.13116D-08	0.46785D-09	0.84376D-09
60	-30	-0.20857D-08	-0.25926D-08	0.50689D-09
60	-29	0.53903D-09	0.29396D-08	-0.24006D-08
60	-28	-0.25816D-08	-0.15190D-08	-0.10626D-08
60	-27	0.11087D-08	0.20053D-08	-0.89665D-09
60	-26	0.96373D-09	0.40365D-08	-0.30728D-08
60	-25	-0.30964D-09	0.56998D-09	-0.87962D-09
60	-24	-0.26082D-09	0.12049D-08	-0.14657D-08
60	-23	0.96187D-10	-0.26684D-08	0.27646D-08
60	-22	0.13262D-08	0.38219D-08	-0.24957D-08
60	-21	0.36631D-09	-0.46549D-08	0.50213D-08
60	-20	-0.15748D-08	0.47165D-10	-0.16220D-08
60	-19	-0.21637D-08	-0.21165D-08	-0.47181D-10
60	-18	-0.51469D-09	-0.26543D-08	0.21396D-08
60	-17	0.10861D-08	0.16382D-08	-0.55213D-09
60	-16	-0.17949D-09	-0.89059D-09	0.71110D-09
60	-15	-0.15896D-08	0.13127D-09	-0.17209D-08
60	-14	0.88393D-09	-0.13718D-08	0.22557D-08
60	-13	0.11455D-08	-0.74640D-09	0.18919D-08
60	-12	-0.60802D-09	-0.31579D-08	0.25499D-08
60	-11	0.21756D-08	0.42679D-08	-0.20923D-08
60	-10	-0.26677D-09	-0.26364D-08	0.23696D-08
60	-9	0.61296D-09	0.21530D-08	-0.15400D-08
60	-8	-0.42761D-09	-0.11297D-08	0.70208D-09
60	-7	-0.20593D-08	-0.25316D-08	0.47225D-09
60	-6	-0.90436D-10	-0.29507D-08	0.28603D-08
60	-5	0.29316D-08	-0.50840D-09	0.34400D-08
60	-4	0.29509D-08	0.54279D-11	0.29455D-08
60	-3	-0.23483D-09	0.28230D-10	-0.26306D-09
60	-2	0.44988D-08	-0.20962D-08	0.65949D-08
60	-1	0.30339D-08	0.22733D-09	0.28066D-08
60	0	0.55763D-09	-0.43711D-09	0.99474D-09
60	1	-0.21584D-08	0.13504D-08	-0.35087D-08
60	2	-0.25921D-08	0.35415D-08	-0.61336D-08
60	3	0.28527D-08	0.29425D-08	-0.89796D-10
60	4	0.25132D-08	0.71391D-08	-0.46259D-08
60	5	0.19224D-08	-0.21465D-08	0.40689D-08
60	6	0.37624D-08	-0.43110D-08	0.80735D-08
60	7	-0.33096D-09	-0.18526D-08	0.15216D-08
60	8	0.13209D-08	0.25776D-08	-0.12567D-08
60	9	-0.14444D-08	0.62251D-09	-0.20669D-08
60	10	-0.21790D-09	0.43547D-09	-0.65337D-09
60	11	-0.11928D-09	0.26528D-08	-0.27721D-08
60	12	0.19093D-08	0.91953D-09	0.98973D-09
60	13	0.23151D-09	-0.51419D-09	0.74570D-09
60	14	0.61202D-09	-0.24719D-08	0.30839D-08
60	15	0.16145D-08	0.10960D-08	0.51843D-09
60	16	-0.15319D-08	-0.33491D-08	0.18172D-08
60	17	-0.33473D-09	-0.49659D-08	0.46312D-08
60	18	0.22665D-09	-0.23156D-08	0.25423D-08
60	19	0.17648D-08	0.35848D-08	-0.18200D-08
60	20	-0.32402D-09	-0.96528D-09	0.64126D-09
60	21	-0.22330D-09	0.11374D-08	-0.13607D-08
60	22	0.15517D-08	0.31923D-08	-0.16406D-08
60	23	0.12287D-08	0.64705D-08	-0.52417D-08
60	24	0.26963D-09	-0.19127D-08	0.21823D-08
60	25	0.11062D-08	0.14109D-08	-0.30473D-09
60	26	0.23474D-08	0.36992D-08	-0.13519D-08
60	27	-0.37904D-08	-0.43367D-08	0.54625D-09
60	28	-0.60458D-09	0.14033D-08	-0.20079D-08
60	29	0.13661D-08	0.20521D-08	-0.68596D-09

```
 60  30   -0.43386D-08   -0.44107D-08    0.72156D-10
 60  31    0.53863D-10    0.39545D-08   -0.39007D-08
 60  32    0.18099D-08   -0.65322D-09    0.24631D-08
 60  33   -0.23961D-08   -0.47283D-08    0.23322D-08
 60  34    0.24070D-08    0.45903D-08   -0.21832D-08
 60  35   -0.48628D-09    0.14297D-08   -0.19160D-08
 60  36   -0.42360D-10    0.87163D-09   -0.91399D-09
 60  37   -0.92577D-09   -0.29002D-08    0.19744D-08
 60  38    0.55293D-09    0.13159D-08   -0.76301D-09
 60  39    0.51645D-09   -0.22431D-08    0.27595D-08
 60  40    0.21455D-09   -0.60066D-09    0.81521D-09
 60  41    0.50222D-09   -0.78934D-09    0.12916D-08
 60  42    0.12289D-08    0.17109D-08   -0.48198D-09
 60  43    0.13255D-08    0.44354D-08   -0.31100D-08
 60  44    0.19997D-08    0.14306D-08    0.56908D-09
 60  45    0.32494D-08    0.41394D-08   -0.89000D-09
 60  46    0.14490D-08    0.11871D-08    0.26189D-09
 60  47    0.10233D-08    0.77945D-09    0.24382D-09
 60  48   -0.25406D-08   -0.44791D-08    0.19385D-08
 60  49    0.28313D-08    0.59407D-08   -0.31094D-08
 60  50    0.16628D-08    0.35671D-08   -0.19043D-08
 60  51   -0.17462D-08   -0.29579D-08    0.12117D-08
 60  52    0.23659D-08    0.33330D-08   -0.96712D-09
 60  53   -0.91780D-09   -0.89012D-09   -0.27683D-10
 60  54    0.27149D-08    0.47513D-08   -0.20365D-08
 60  55    0.18673D-08    0.23881D-08   -0.52080D-09
 60  56   -0.78634D-09   -0.14553D-08    0.66891D-09
 60  57   -0.12148D-08   -0.17442D-08    0.52939D-09
 60  58   -0.10528D-08   -0.14409D-08    0.38809D-09
 60  59   -0.20947D-08   -0.23204D-08    0.22576D-09
 60  60    0.19504D-08    0.42307D-08   -0.22803D-08
MEAN, STDV, VARI=      0.91208D-10     0.22501D-08     0.22426D-08
MEAN COLL ERR=      0.00000D+00 COEFF. STDV.      0.28349D-08

 61 -61   -0.33387D-09    0.00000D+00   -0.33387D-09
 61 -60   -0.22644D-08    0.00000D+00   -0.22644D-08
 61 -59   -0.74328D-09    0.00000D+00   -0.74328D-09
MEAN, STDV, VARI=     -0.27167D-10     0.21617D-09     0.21699D-09
MEAN COLL ERR=      0.00000D+00 COEFF. STDV.      0.00000D+00


 DEG,      STDV OBS-PRED    STDV-COEFFICIENTS
   3   0.1669169D-10   0.0000000D+00
   4   0.5714272D-10   0.0000000D+00
   5   0.4633225D-10   0.0000000D+00
   6   0.1150253D-09   0.0000000D+00
   7   0.1034789D-09   0.0000000D+00
   8   0.1676590D-09   0.0000000D+00
   9   0.1925885D-09   0.0000000D+00
  10   0.2073778D-09   0.0000000D+00
  11   0.2678199D-09   0.0000000D+00
  12   0.2054967D-09   0.0000000D+00
  13   0.2872450D-09   0.0000000D+00
  14   0.2733462D-09   0.0000000D+00
  15   0.3240719D-09   0.0000000D+00
  16   0.2604716D-09   0.0000000D+00
  17   0.3762456D-09   0.0000000D+00
  18   0.2637849D-09   0.0000000D+00
  19   0.3481893D-09   0.0000000D+00
  20   0.3532846D-09   0.0000000D+00
  21   0.3138026D-09   0.0000000D+00
  22   0.3007600D-09   0.0000000D+00
  23   0.2992825D-09   0.0000000D+00
```

```
  24   0.3398748D-09   0.0000000D+00
  25   0.1061678D-08   0.1077005D-07
  26   0.8871900D-09   0.8917749D-08
  27   0.1212142D-08   0.7126836D-08
  28   0.1141220D-08   0.8888525D-08
  29   0.1210495D-08   0.7753920D-08
  30   0.1199174D-08   0.7782810D-08
  31   0.1375060D-08   0.7128380D-08
  32   0.1350909D-08   0.6770942D-08
  33   0.1332935D-08   0.6876457D-08
  34   0.1323530D-08   0.7557858D-08
  35   0.1049923D-08   0.7171514D-08
  36   0.1167867D-08   0.6257407D-08
  37   0.1149589D-08   0.6222925D-08
  38   0.1177703D-08   0.5477743D-08
  39   0.1132304D-08   0.5554505D-08
  40   0.1321917D-08   0.4920234D-08
  41   0.1308930D-08   0.5008565D-08
  42   0.1368833D-08   0.5033405D-08
  43   0.1213304D-08   0.4547051D-08
  44   0.1159546D-08   0.4376185D-08
  45   0.1354511D-08   0.4526116D-08
  46   0.1386464D-08   0.4634816D-08
  47   0.1504823D-08   0.4412879D-08
  48   0.1571695D-08   0.3971595D-08
  49   0.1296415D-08   0.3541803D-08
  50   0.1644465D-08   0.3971641D-08
  51   0.1913897D-08   0.3534316D-08
  52   0.1748287D-08   0.3499428D-08
  53   0.1774672D-08   0.3818174D-08
  54   0.1863751D-08   0.3539692D-08
  55   0.1860052D-08   0.3222357D-08
  56   0.2114715D-08   0.3439972D-08
  57   0.2212071D-08   0.3328182D-08
  58   0.2096276D-08   0.2899005D-08
  59   0.2391840D-08   0.3090424D-08
  60   0.2242639D-08   0.2834854D-08
  61   0.2169945D-09   0.0000000D+00
 END OF COMPUTATIONS (T/F)

TIME USED=23361.219 SEC, ELAPSED TIME = 23407.499 SEC
TOTAL CPU TIME USED=    49600.139 SEC
 GEOCOL TERMINATED AT:
Fri Dec  3 05:10:54 2004
```